

Cite this: *Phys. Chem. Chem. Phys.*, 2011, **13**, 8094–8111

www.rsc.org/pccp

PERSPECTIVE

## High-dimensional *ab initio* potential energy surfaces for reaction dynamics calculations

Joel M. Bowman,\* Gábor Czakó and Bina Fu

Received 30th November 2010, Accepted 17th January 2011

DOI: 10.1039/c0cp02722g

There has been great progress in the development of potential energy surfaces (PESs) for reaction dynamics that are fits to *ab initio* energies. The fitting techniques described here explicitly represent the invariance of the PES with respect to all permutations of like atoms. A review of a subset of dynamics calculations using such PESs (currently 16 such PESs exist) is then given. Bimolecular reactions of current interest to the community, namely,  $\text{H} + \text{CH}_4$  and  $\text{F} + \text{CH}_4$ , are focused on. Unimolecular reactions are then reviewed, with a focus on the photodissociation dynamics of  $\text{H}_2\text{CO}$  and  $\text{CH}_3\text{CHO}$ , where so-called “roaming” pathways have been discovered. The challenges for electronically non-adiabatic reactions, and associated PESs, are presented with a focus on the  $\text{OH}^* + \text{H}_2$  reaction. Finally, some thoughts on future directions and challenges are given.

### I. Introduction

Theoretical and experimental research in chemical reaction dynamics has undergone major advances in the recent past, moving from the very detailed studies of atom plus diatom and some triatomic reactions to truly polyatomic systems, consisting of roughly ten atoms. Perhaps the biggest change (and challenge) in such polyatomic systems is the large number of possible reaction products, and in the case of radical

reactions and unimolecular dissociations, the “ruggedness”, *i.e.*, multiple minima and barriers separating them, of the potential energy surface. In addition, even for direct reactions, without stable intermediates, the investigation of mode-specific chemistry, one of the hall mark areas of research uncovered in atom and triatomic reaction dynamics, has also received considerable attention and has uncovered some surprising results.<sup>1–5</sup>

The theoretical/computational approach to polyatomic reaction dynamics is challenged in two major ways. The first is the potential energy surface, which as noted above may be quite complicated. The second challenge is the dynamics, where currently at least, the application of essentially exact

Department of Chemistry and Cherry L. Emerson Center for Scientific Computation, Emory University, Atlanta, GA 30322.  
E-mail: jmbowma@emory.edu



Joel M. Bowman

Joel Bowman received his A. B. degree from the University of California, Berkeley, where he was elected to Phi Beta Kappa. He received his PhD from Caltech in 1975. He is a Fellow of the American Physical Society and the American Association for the Advancement of Science and is the Samuel Candler Dobbs Professor of Chemistry at Emory University. In 2010 he was a Visiting Fellow at Magdalen College, Oxford University. His research

interests include chemical reaction dynamics, development of potential energy surfaces, vibrational analysis of molecules and clusters and method development.



Gábor Czakó

Gábor Czakó received his PhD in theoretical chemistry at Eötvös University, Budapest, Hungary in 2007 and he is currently a postdoctoral researcher in the Department of Chemistry at Emory University, Atlanta, GA, USA. His research interests involve first-principles reaction dynamics and (ro)vibrational spectroscopy as well as high-accuracy *ab initio* thermochemistry. He received silver medal in the 31st International Chemistry Olympiad, Bangkok, Thailand, and several national awards in Hungary.

quantum methods to atom-diatom reactions, have not yet been extended to general polyatomic reactions. Of these two aspects/challenges we might make the provocative claim that the potential is of primary importance. Indeed, it is obvious that the “wrong potential is guaranteed to give the wrong answer”, when used in an exact dynamics calculation, or more likely in an approximate, but well-benchmarked calculation. Indeed much experience has shown that an accurate potential, even when used in a less-than-exact dynamics calculation, *e.g.*, the ubiquitous quasiclassical trajectory calculations, or well-tested tunneling corrected transition state theory does very often give accurate results for say final state distributions or the thermal rate constant, respectively.

The potential is, in the Born–Oppenheimer approximation, the sum of the electronic energy plus the nuclear repulsion energy. Thus, in principle it can be calculated “as needed” for any dynamical treatment of the nuclei. This is the Direct-Dynamics approach. When used, as it almost always is at present, with a classical treatment of the dynamics, this approach is referred to *Ab initio* Molecular Dynamics (AIMD). This generally means running classical trajectories and obtaining the potential and its gradient by direct calls to electronic structure codes at each time step. There is a huge literature of applications of this approach, owing to its obvious appeal and generality. It has been used extensively in studies of reaction dynamics and the reader is referred to ref. 6–13 for some examples. However, even with this most efficient treatment of the dynamics (compared to a quantum treatment), AIMD is extremely cpu intensive. To illustrate this, consider a recent study of AIMD for H<sub>2</sub>CO dissociation to H<sub>2</sub> + CO, starting at the molecular saddle point, by some of the best practitioners in this field.<sup>13</sup> They reported the time to propagate a single trajectory, using the popular velocity-Verlet method with a low level of *ab initio* theory/basis, *i.e.*, Hartree–Fock/6-31G(d,p), to be in the range of 680 s for 240 gradient calls on a 3.2 GHz Xeon processor. They proposed and tested a Hessian-based method to integrate the same trajectory, which took only 173 s, which is a very substantial reduction in the cpu time. However, this is still a substantial amount of cpu time, especially given the very low level of *ab initio* theory. As is well known, the cpu effort of electronic structure methods grows non-linearly with increasing basis and also with the accuracy of the method. For example from

our own work on H<sub>2</sub>CO a *single* energy using the CCSD(T)/aug-cc-pVTZ method/basis takes roughly 200 s on a similar workstation, using the very efficient MOLPRO software.<sup>14</sup> So clearly AIMD with this method would be totally unfeasible. For CH<sub>3</sub>CHO a single energy calculation using this method and basis takes roughly 2500 s, when run with MOLPRO in 4-way parallel on a single core.

Based on the above, it is understandable that AIMD is generally limited to fairly short propagation times, *i.e.*, ten picoseconds or less, a fairly small number of trajectories, *e.g.*, less than 1000, and to the use of fairly low-levels of electron structure methods, *e.g.*, Density Functional Theory. (Note we include Density Functional Theory under the “AIMD” umbrella, even though its implementation involves semi-empiricism.) These limitations notwithstanding, the AIMD method is a powerful means to investigate and uncover mechanisms of reaction dynamics with multiple pathways, some of which may be quite surprising and insightful. (This statement applies in general to the quasiclassical trajectory method, whether using direct dynamics or a fitted potential energy surface.)

It is however, frustrating in our opinion, that the very costly *ab initio* data, is essentially discarded after the trajectories are performed. Making use of AIMD data was a major motivation for the fitting methods we will describe later. Next, we discuss other strategies that fall between AIMD and fitting *ab initio* energies.

One strategy is to use much more efficient semi-empirical electronic structure methods in Direct Dynamics. Generally these methods are not sufficiently accurate to be of much use in reaction dynamics calculations. With this mind, Truhlar and co-workers<sup>15</sup> suggested replacing the “reaction parameters” that typically come with semi-empirical software with “Specific Reaction Parameters” that are optimized for say the barrier height and reaction energy of a given reaction. This is an important advance for simple reactions, with a single set of products,<sup>15–18</sup> and we will return to this approach briefly when we discuss the F + CH<sub>4</sub> reaction. The “Empirical Valence Bond” method,<sup>19,20</sup> and recent extensions,<sup>21</sup> is another example of this approach. However, even these methods, which are highly simplified and of limited applicability, are still quite cpu intensive if one needs to propagate for tens or hundreds of picoseconds and/or needs to run tens of thousands of trajectories to obtain a sufficient sampling of the initial phase space.

In view of the limitations of the Direct Dynamics/AIMD approach, the existence of analytical expressions for the potential energy surface is an important tool (and a continuing goal) in the field of reaction dynamics. Such representations are ubiquitous for atom plus diatom reactions. For these systems, it was possible to obtain a highly accurate representation of the potential, which hereafter, we shall denote as the PES, with as few as 1000 electronic energies. Excellent reviews of fitting methods along with applications up to 1989 are given by Schatz<sup>22</sup> and more recently by Ho and Rabitz.<sup>23</sup> Perhaps the current state-of-the-art is represented by a PES published in 2007 by Honvault and Guo and co-workers for the H + O<sub>2</sub> reaction,<sup>24</sup> where more than 18 000 electronic energies were fit using a 3d spline.



**Bina Fu**

*Bina Fu is a Postdoctoral Research Fellow in the chemistry department at Emory University. She received her PhD in the State Key Laboratory of Molecular Reaction Dynamics at the Dalian Institute of Chemical Physics of the Chinese Academy of Sciences in July 2009. Her research interests involve ab initio potential energy surface calculations and classical and quantum dynamical studies of polyatomic chemical reactions.*

Unfortunately, this and other methods used to fit three-atom reactions do not scale well for larger reaction systems. Other approaches have been developed to represent high-dimensional PESs for both reactive and non-reactive systems with more than 4 atoms. Perhaps the first significant step in this direction was taken by Collins and co-workers,<sup>25</sup> who developed a method based on interpolating numerous local force fields, and which has been applied to a number of polyatomic reactions. Other methods employing many body methods, “moving least-squares”, *etc.* also appear promising for polyatomic reaction.<sup>26–29</sup>

Progress in our group in developing PESs for high dimensional and complicated reactive systems is based on employing a representation of the PES that is explicitly invariant with respect to all permutations of like atoms. This approach has been described in detail in a recent review by Braams and Bowman,<sup>30</sup> and so will only be briefly reviewed here. A large number of such permutationally invariant PESs, which we denote by PI PESs, have been reported for reaction dynamics. Table 1 contains this current list along with corresponding citations.

The goal of this Perspective is to present some details of the theory and practice of PI PESs and then to give a sample of applications to reaction dynamics calculations of bimolecular and unimolecular reactions, and one electronically non-adiabatic reaction of current interest. In the next section, we describe the PI PES fitting method and illustrate the method by describing the PI PES for the H + CH<sub>4</sub> reaction. In Section III we review dynamics calculations, and some rate constant calculations, for this reaction and also for the F + CH<sub>4</sub> and HO<sub>2</sub> + NO reactions. Then we consider two intensively studied photodissociation reactions, H<sub>2</sub>CO and CH<sub>3</sub>CHO. We conclude with very recent dynamics calculations of the electronically non-adiabatic reactive and non-reactive quenching of OH\* by H<sub>2</sub>. In all of these examples PI PESs have been developed and employed in the dynamics calculations. These will be focused on; however, PESs developed by others, which have been used to study some of these reactions will also be described. The final section will present a summary, conclusions and some comments on future directions.

**Table 1** *Ab initio* PESs for reaction dynamics developed using permutationally invariant bases

Reaction	Reference
CH <sub>5</sub> <sup>+</sup> → H <sub>2</sub> + CH <sub>3</sub> <sup>+</sup>	71
H <sub>5</sub> <sup>+</sup> → H <sub>2</sub> + H <sub>3</sub> <sup>+</sup>	166
H' + CH <sub>4</sub> → HH' + CH <sub>3</sub> , H + CH <sub>3</sub> H'	44
F + CH <sub>4</sub> (CHD <sub>3</sub> ) → HF + CH <sub>3</sub> (HF + CD <sub>3</sub> , DF + CHD <sub>2</sub> )	88
NO <sub>2</sub> + OH → [HOONO(isomers), HONO <sub>2</sub> ] → NO + HO <sub>2</sub>	117
C + C <sub>2</sub> H <sub>2</sub> → <i>l</i> -C <sub>3</sub> H, <i>c</i> -C <sub>3</sub> H + H, C <sub>3</sub> + H <sub>2</sub>	129
CHOCH <sub>2</sub> CHO (malonaldehyde) H-atom transfer	41
CH <sub>3</sub> CHO → CH <sub>4</sub> + CO, CH <sub>3</sub> + HCO, C <sub>2</sub> H <sub>2</sub> + H <sub>2</sub> O, <i>etc.</i>	141 and 136
C <sub>2</sub> H <sub>3</sub> → H + C <sub>2</sub> H <sub>2</sub> and isomerization	165
C <sub>3</sub> H <sub>5</sub> → H + C <sub>3</sub> H <sub>4</sub> (isomers), CH <sub>3</sub> + C <sub>2</sub> H <sub>2</sub>	42
H <sub>2</sub> O + D <sub>2</sub> O → 2HDO	164
CH <sub>2</sub> CH <sub>2</sub> OH → OH + CH <sub>2</sub> CH <sub>2</sub> , H <sub>2</sub> O + C <sub>2</sub> H <sub>3</sub> , <i>etc.</i>	144
CH <sub>5</sub> <sup>+</sup> (+Cs) → [CH <sub>5</sub> ]* → H <sub>2</sub> + CH <sub>3</sub> , H + CH <sub>4</sub>	69 and 70
H <sub>3</sub> O <sup>+</sup> (+Cs) → [H <sub>3</sub> O]* → H <sub>2</sub> + OH, H <sub>2</sub> O + H	160
OH + H <sub>2</sub> → H <sub>2</sub> O + H	158
OH* + H <sub>2</sub> → H <sub>2</sub> O + H	158

## II. Permutationally invariant potential energy surfaces

To begin this section we note that the PI PESs listed in Table 1 were obtained by fitting 10<sup>4</sup>–10<sup>5</sup> electronic energies that span an energy range up to roughly 4 eV above a global minimum. That one can obtain accurate global PESs for large systems with only 10<sup>4</sup>–10<sup>5</sup> energies is perhaps quite surprising, given the high dimensionality, *d*, of the space spanned. For 6 atoms the space is 12d and for 9 atoms it is 21d. Clearly in these two cases 50 000 energies represents only 2.5 and 1.7 energies per degree of freedom in a direct-product sense.

The aspect of the fitting that enables us to obtain PESs with so few energies is to explicitly exploit the property that the PES must be invariant with respect to all permutations of identical atoms. (And of course to note that many reaction systems of interest contain identical atoms, *e.g.*, H atoms.) Due to this permutational symmetry, much of the configuration space is redundant and it is this fact that is exploited to reduce the size of the electronic energy database.

Below we briefly describe the development of fitting bases that are explicitly permutationally invariant and indicate some of the important consequences of using these. A much more detailed discussion of these is given elsewhere.<sup>30</sup>

Before doing this, we note that the importance of permutational invariance of PESs has been recognized for some time, *e.g.*, in the classic book on PESs by Murrell *et al.*<sup>31</sup> It was also incorporated by us in the construction of a full dimensional global PESs for C<sub>2</sub>H<sub>2</sub>, which was able to describe the isomerization of acetylene to vinylidene,<sup>32</sup> and later the global PES for unimolecular dissociation of formaldehyde.<sup>33</sup> In both cases, permutational symmetry was incorporated by simply replicating electronic energies for permutationally equivalent configurations for both C<sub>2</sub>H<sub>2</sub> and H<sub>2</sub>CO and thereby to quadruple and double, respectively, the data sets. This approach did produce PESs that are numerically invariant with respect to permutations, however, the number of terms in the representation had to be large in order to represent the enlarged data set. Clearly, such an approach cannot be used for a molecule such as CH<sub>5</sub><sup>+</sup>, where the order of the permutation group is 5! = 120, and thus the size of a replicated data set would be of the order of 10<sup>6</sup>.

Obviously, what is needed is a general approach to incorporate permutational invariance directly into the PES representation, by using a fitting basis that is permutationally invariant. The implementation of this approach is not trivial. Some steps in this direction were made by Murrell *et al.*<sup>31</sup> They noted that an invariant fitting basis with this property can be represented in terms of what they termed an integrity basis. Explicit expressions for such a basis for triatomic molecules and for the special case of 4 identical atoms were given.<sup>34</sup> The variables chosen for this basis were point-group, symmetry-adapted internuclear distances. The techniques they used to generate this basis are in their words “rather tedious” even for the case of 3 identical atoms. More recently Cassam-Chenaï and Patras elaborated on the Murrell *et al.* approach for XY<sub>4</sub> molecules and presented an examples of invariant bases up to fairly high order.<sup>35</sup> In very recent and impressive work by Opalka and Domcke, permutationally invariant bases

were used to describe PESs for the triply-degenerate ground state of  $\text{CH}_4^+$ .<sup>36</sup>

We have described two general approaches to obtain PI bases for molecules with more than four identical atoms.<sup>30,37</sup> In both approaches, the variables are all the internuclear distances, actually Morse variables, described below. These variables form a closed set under permutations and although this is a redundant set of variables, it is a set that uniquely specifies the geometry when transforming from Cartesian coordinates. The more powerful and efficient approach, makes use of results and software from invariant polynomial theory/computation, as described below. The second approach, although less elegant and efficient, is more pedagogical and so we describe it here.

To begin, we use, as in the earlier work on  $\text{C}_2\text{H}_2$ , Morse-like variables  $y_{ij}$  instead of the internuclear distances. These are given by  $y_{ij} = \exp(-r_{ij}/a)$ , where  $a$  is fixed (between 2 and 3 bohr). Then the PES is represented in terms of all  $n(n-1)/2$  such variables, where  $n$  is the number of atoms, by<sup>30,37,38</sup>

$$V = \sum_{n=0}^N C_n S(y_{12}^{n_1} y_{13}^{n_2} y_{14}^{n_3} \cdots y_{23}^{n_4} y_{24}^{n_5} \cdots), \quad (1)$$

**Table 2** Symmetrized monomial bases for  $A_3$  molecules

Atom Labels	Monomial	Normal Order
1 2 3	$y_{12}^a y_{13}^b y_{23}^c$	$y_{12}^a y_{13}^b y_{23}^c$
2 1 3	$y_{12}^a y_{23}^b y_{13}^c$	$y_{12}^a y_{13}^b y_{23}^c$
3 2 1	$y_{23}^a y_{13}^b y_{12}^c$	$y_{12}^a y_{13}^b y_{23}^c$
1 3 2	$y_{13}^a y_{12}^b y_{23}^c$	$y_{12}^a y_{13}^b y_{23}^c$
3 1 2	$y_{13}^a y_{23}^b y_{12}^c$	$y_{12}^a y_{13}^b y_{23}^c$
2 3 1	$y_{23}^a y_{12}^b y_{13}^c$	$y_{12}^a y_{13}^b y_{23}^c$
Symmetrized term: $y_{12}^a y_{13}^b y_{23}^c + y_{12}^a y_{13}^b y_{23}^c + \cdots + y_{12}^a y_{13}^b y_{23}^c + y_{12}^a y_{13}^b y_{23}^c$		

**Table 3** Symmetrized monomial bases for  $A_2B_2$  molecules

Atom Labels	Monomial	Normal Order
1 2 3 4	$y_{12}^a y_{13}^b y_{14}^c y_{23}^d y_{24}^e y_{34}^f$	$y_{12}^a y_{13}^b y_{14}^c y_{23}^d y_{24}^e y_{34}^f$
2 1 3 4	$y_{12}^a y_{23}^b y_{24}^c y_{13}^d y_{14}^e y_{34}^f$	$y_{12}^a y_{13}^b y_{14}^c y_{23}^d y_{24}^e y_{34}^f$
1 2 4 3	$y_{12}^a y_{14}^b y_{13}^c y_{24}^d y_{23}^e y_{34}^f$	$y_{12}^a y_{13}^b y_{14}^c y_{23}^d y_{24}^e y_{34}^f$
2 1 4 3	$y_{12}^a y_{24}^b y_{23}^c y_{14}^d y_{13}^e y_{34}^f$	$y_{12}^a y_{13}^b y_{14}^c y_{23}^d y_{24}^e y_{34}^f$
Symmetrized term: $y_{12}^a y_{13}^b y_{14}^c y_{23}^d y_{24}^e y_{34}^f + \cdots + y_{12}^a y_{13}^b y_{14}^c y_{23}^d y_{24}^e y_{34}^f$		

**Table 4** Symmetrized monomial bases for  $A_3B_2$  molecules

Atom Labels	Monomial	Normal Order
1 2 3 4 5	$y_{12}^a y_{13}^b y_{14}^c y_{15}^d y_{23}^e y_{24}^f y_{25}^g y_{34}^h y_{35}^i y_{45}^j$	$y_{12}^a y_{13}^b y_{14}^c y_{15}^d y_{23}^e y_{24}^f y_{25}^g y_{34}^h y_{35}^i y_{45}^j$
2 1 3 4 5	$y_{12}^a y_{23}^b y_{24}^c y_{25}^d y_{13}^e y_{14}^f y_{15}^g y_{34}^h y_{35}^i y_{45}^j$	$y_{12}^a y_{13}^b y_{14}^c y_{15}^d y_{23}^e y_{24}^f y_{25}^g y_{34}^h y_{35}^i y_{45}^j$
3 2 1 4 5	$y_{23}^a y_{13}^b y_{34}^c y_{35}^d y_{12}^e y_{24}^f y_{25}^g y_{14}^h y_{15}^i y_{45}^j$	$y_{12}^a y_{13}^b y_{14}^c y_{15}^d y_{23}^e y_{24}^f y_{25}^g y_{34}^h y_{35}^i y_{45}^j$
1 3 2 4 5	$y_{13}^a y_{12}^b y_{14}^c y_{15}^d y_{23}^e y_{34}^f y_{35}^g y_{24}^h y_{25}^i y_{45}^j$	$y_{12}^a y_{13}^b y_{14}^c y_{15}^d y_{23}^e y_{24}^f y_{25}^g y_{34}^h y_{35}^i y_{45}^j$
3 1 2 4 5	$y_{13}^a y_{23}^b y_{34}^c y_{35}^d y_{12}^e y_{14}^f y_{15}^g y_{24}^h y_{25}^i y_{45}^j$	$y_{12}^a y_{13}^b y_{14}^c y_{15}^d y_{23}^e y_{24}^f y_{25}^g y_{34}^h y_{35}^i y_{45}^j$
2 3 1 4 5	$y_{23}^a y_{12}^b y_{24}^c y_{25}^d y_{13}^e y_{34}^f y_{35}^g y_{14}^h y_{15}^i y_{45}^j$	$y_{12}^a y_{13}^b y_{14}^c y_{15}^d y_{23}^e y_{24}^f y_{25}^g y_{34}^h y_{35}^i y_{45}^j$
1 2 3 5 4	$y_{12}^a y_{13}^b y_{15}^c y_{14}^d y_{23}^e y_{25}^f y_{24}^g y_{35}^h y_{34}^i y_{45}^j$	$y_{12}^a y_{13}^b y_{14}^c y_{15}^d y_{23}^e y_{24}^f y_{25}^g y_{34}^h y_{35}^i y_{45}^j$
2 1 3 5 4	$y_{12}^a y_{23}^b y_{25}^c y_{24}^d y_{13}^e y_{15}^f y_{14}^g y_{35}^h y_{34}^i y_{45}^j$	$y_{12}^a y_{13}^b y_{14}^c y_{15}^d y_{23}^e y_{24}^f y_{25}^g y_{34}^h y_{35}^i y_{45}^j$
3 2 1 5 4	$y_{23}^a y_{13}^b y_{35}^c y_{34}^d y_{12}^e y_{25}^f y_{24}^g y_{15}^h y_{14}^i y_{45}^j$	$y_{12}^a y_{13}^b y_{14}^c y_{15}^d y_{23}^e y_{24}^f y_{25}^g y_{34}^h y_{35}^i y_{45}^j$
1 3 2 5 4	$y_{13}^a y_{12}^b y_{15}^c y_{14}^d y_{23}^e y_{35}^f y_{34}^g y_{25}^h y_{24}^i y_{45}^j$	$y_{12}^a y_{13}^b y_{14}^c y_{15}^d y_{23}^e y_{24}^f y_{25}^g y_{34}^h y_{35}^i y_{45}^j$
3 1 2 5 4	$y_{13}^a y_{23}^b y_{35}^c y_{34}^d y_{12}^e y_{15}^f y_{14}^g y_{25}^h y_{24}^i y_{45}^j$	$y_{12}^a y_{13}^b y_{14}^c y_{15}^d y_{23}^e y_{24}^f y_{25}^g y_{34}^h y_{35}^i y_{45}^j$
2 3 1 5 4	$y_{23}^a y_{12}^b y_{25}^c y_{24}^d y_{13}^e y_{35}^f y_{34}^g y_{15}^h y_{14}^i y_{45}^j$	$y_{12}^a y_{13}^b y_{14}^c y_{15}^d y_{23}^e y_{24}^f y_{25}^g y_{34}^h y_{35}^i y_{45}^j$
Symmetrized basis: $y_{12}^a y_{13}^b y_{14}^c y_{15}^d y_{23}^e y_{24}^f y_{25}^g y_{34}^h y_{35}^i y_{45}^j + \cdots + y_{12}^a y_{13}^b y_{14}^c y_{15}^d y_{23}^e y_{24}^f y_{25}^g y_{34}^h y_{35}^i y_{45}^j$		

where  $S$  is a ‘‘symmetrization’’ operator, which we describe shortly, and where  $C_n$  are the unknown linear coefficients, which are determined by standard linear least-squares fitting methods. The overall maximum power of the symmetrized monomials is fixed at typically 5 or 6, and  $N$  represents the number of terms in the summation. Illustrations of the number of terms will be given below.

The symmetrization operator  $S$  is best explained by referring to Table 2, Table 3 and Table 4, where all permutations of like atoms for the three molecule types indicated are given, along with the corresponding mapping of internuclear distances. The action of each permutation on a ‘‘seed’’ monomial follows and the sum of all transformed monomials is indicated in the last row of each table. This summed term is clearly invariant under all permutations and serves as the desired ‘‘symmetrized sum-of-monomials’’ basis function. As can be seen, the size of the resulting invariant basis function approaches the order of the corresponding symmetric group in the limit of large total polynomial order. However, the number of terms in the resulting sum, eqn (1), which can be obtained from the Molien series, is reduced compared to not using symmetrization. Further, the reduction increases significantly as the order of the relevant symmetric group increases. This is shown in Table 5 for a few examples. The case where all atoms are different gives the number of terms without symmetrization,

**Table 5** Number of terms for indicated molecules versus total order indicated

Molecule	5	6	7	8
$A_3$	16	23	31	41
$A_2B$	34	50	70	95
ABC	56	84	120	165
$A_4$	40	72	120	195
$A_3B$	103	196	348	590
$A_2B_2$	153	291	519	882
$A_2BC$	256	502	918	1589
ABCD	462	924	1716	3003
$A_5$	64	140	289	580
$A_4B$	208	495	1101	2327
$A_3B_2$	364	889	2022	4343
$A_3BC$	636	1603	3737	8163
$A_2B_2C$	904	2304	5416	11910
$A_2BCD$	1632	4264	10208	22734
ABCDE	3003	8008	19448	43758

for a given total polynomial order. As seen, the reduction is roughly a factor of 4 for triatomics, factors of 2–15 for tetraatomics, and as much as roughly 100 for a pentatomic, *e.g.*,  $\text{H}_5^+$  and  $\text{CH}_5^+$ . For  $\text{H}_5\text{O}_2^+$ , where the order of the symmetric group is  $5! = 240$  the number of coefficients to determine without exploiting symmetry would be so large as to make solving the linear algebra problem prohibitive and definitely prohibitive for  $(\text{H}_2\text{O})_3$  where the order is 4320. Exploiting this symmetry, PESs have been developed for all of these examples.

The fitting basis we use most often is a more sophisticated and efficient one, based on invariant polynomial theory.<sup>39</sup> In this approach the expression for the PI PES is<sup>30,38</sup>

$$V(\mathbf{y}) = \sum_{n=0}^N h_n[\mathbf{p}(\mathbf{y})]q_n(\mathbf{y}), \quad (2)$$

where  $h_n$  is a polynomial of the  $\mathbf{p}(\mathbf{y})$ , the so-called primary invariant polynomials, and  $q_n(\mathbf{y})$  are secondary invariant polynomials and  $\mathbf{y}$  represents the set of variables  $y_{ij}$ . Computational software MAGMA<sup>40</sup> was used to generate these polynomials for up to ten atoms. More details about these bases can be found elsewhere;<sup>30</sup> the library of fitting bases is available for download at <http://iopshell.usc.edu/downloads/ezpes/>. Software using the more straightforward monomial symmetrization has also been developed,<sup>37</sup> and is available at <http://www.mcs.anl.gov/msa>.

Next, we describe the electronic energy database for fitting. As noted above we often start with a PES based on a low-level electronic structure method, *e.g.*, DFT and a small basis. Data for this PES are typically obtained using AIMD calculations to sample the configuration space. The AIMD calculations are typically done at several total energies and starting from several initial configurations. The database of configurations for fitting is pruned by removing near-duplicate configurations. (For this purpose we have designed tests for similarity that involve only permutationally invariant functions of internuclear distances, so we recognize the similarity between configurations in arbitrary relative position and with arbitrary re-labeling of nuclei.) We then carry out a quasi-Newton search for all stationary configurations on the surface and then additional *ab initio* electronic energies are obtained in the vicinity of these configurations. (The location of stationary points on the initial PES very often produces surprisingly accurate results for both minima and saddle points.) These data are fit and then additional molecular dynamics and/or Diffusion Monte Carlo calculations of the ground state vibrational wavefunction at one or more minima are done on this version of the PES. Based on this refined initial PES higher-level *ab initio* calculations, often CCSD(T) with an aug-cc-pVTZ basis, are done at a subset of the configurations used in the fit of the lower-level PES. For example, this approach was used very effectively to obtain a full-dimensional PES for H-atom transfer in malonaldehyde, using a very expensive and accurate composite *ab initio* method.<sup>41</sup>

Also, we note that the dipole moment can and has been calculated and fit, mainly for applications to IR spectroscopy. However, that is not the focus of this article and so we omit details of this here.

For reactive PESs, which are the focus of this article, the electronic database described above is supplemented with electronic energies of the various fragments. For consistency, the electronic energies of the fragments are obtained with the same method and basis as for the supermolecular system. For example, in the recent study of the unimolecular dissociation of the allyl radical,<sup>42</sup> electronic energies for the  $\text{H} + \text{C}_3\text{H}_4$  (including isomers) and  $\text{CH}_3 + \text{C}_2\text{H}_2$  (including the vinylidene isomer) channels were included in the complete database. These fragment data are placed at sensible distances in the relevant dissociation coordinate. Of course, data for near dissociation configurations are also included in the database, and then the entire database of energies was fit using the PI bases, using standard least squares fitting software.

In cases where fragment channels contain open-shell species, *e.g.*,  $\text{CH}_3 + \text{HCO}$  from the dissociation of  $\text{CH}_3\text{HCO}$ , this presents well-known difficulties for single reference methods such as CCSD(T). Of course, very often the isolated fragments themselves, can be described using a single reference method, and so one expedient approach around the multi-reference character of the PES in the near dissociation region to such fragments is to interpolate through the problematic regions. This can of course be problematic procedure, which at the very least must be checked by comparing the PES in the multi-reference region to rigorous calculations obtained with a multi-reference method. A more robust approach, which has been implemented for  $\text{CH}_3\text{CHO}$ , is to add electronic energies from a multi-reference method, such as MRCI, to the database of electronic energies. Of course care must be taken to apply a sensible shift to these energies to make them compatible with say CCSD(T) energies.

The fitting, as noted already, is linear least squares and so the fit does not reproduce the data exactly. However, by suitable weighting, *etc.* it possible to achieve a fitting accuracy that is well within the intrinsic errors of the electronic structure method and basis used. The root mean square fitting error, as expected, depends on the complexity of potential surface and the energy span of the data being fit. The reader is referred to the references given in Table 1 for more details for each system listed there.

One relevant example of the accuracy and properties of a PI PES obtained with the methods just described is for the  $\text{H} + \text{CH}_4 \rightarrow \text{H}_2 + \text{CH}_3$  (and isotopologs) reaction. Table 6 contains a comparison of the geometries and normal mode frequencies of the abstraction and high-energy exchange saddle points for two fitted PESs,<sup>43,44</sup> denoted ZBB3 and ZBB2, with results obtained from direct CCSD(T)/aug-cc-pVTZ *ab initio* calculations. The PESs are fits to slightly different databases of roughly 20 000 CCSD(T)/aug-cc-pVTZ energies; ZBB3 contains additional data in the vicinity of the exchange saddle point. Focusing on the ZBB2 PES, we see very good agreement with the direct *ab initio* results for the abstraction saddle point and good agreement for the high-energy exchange saddle point. As expected, ZBB3 is more accurate for the latter saddle point, at the cost of somewhat reduced accuracy for the former one. To the best of our knowledge these are the only global PESs that contain the exchange saddle point. This is also an indication that the PESs realistically describe the high-energy regions of relevance to several experiments that will be briefly

**Table 6** CH<sub>5</sub> abstraction (ABSP) and exchange (EXSP) saddle point geometries, energies, and harmonic frequencies (cm<sup>-1</sup>) on the ZBB2, ZBB3 potential energy surfaces and directly from *ab initio* calculations

	CH <sub>5</sub> ABSP			CH <sub>5</sub> EXSP		
	<i>ab initio</i>	ZBB2	ZBB3	<i>ab initio</i>	ZBB2	ZBB3
Energy (kcal/mol)	14.67	14.86	14.78	37.5	30.84	36.37
Mode 01	1437i	1375i	1320i	1537i	1385i	1687i
Mode 02	531	510	440	836	1008	948
Mode 03	531	510	440	836	1008	948
Mode 04	1082	1013	1062	1302	1196	1373
Mode 05	1126	1057	1078	1348	1196	1373
Mode 06	1126	1057	1078	1348	1491	1393
Mode 07	1445	1442	1434	1377	1491	1440
Mode 08	1445	1442	1434	1377	1530	1440
Mode 09	1779	1768	1726	1540	1637	1607
Mode 10	3073	3059	3104	3016	2924	2966
Mode 11	3220	3245	3289	3199	3432	3350
Mode 12	3220	3245	3289	3199	3432	3350
$R_{CH}$ (Å)	1.0854	1.0853	1.0843	1.0863	1.0629	1.0822
$R_{CH'}$ (Å)	1.3991	1.4015	1.4086	1.3612	1.4495	1.3645
$R_{CH'H'}$ (Å)	0.8970	0.9027	0.9016			
$\angle HCH'$ (deg)	103.1	102.8	102.8			

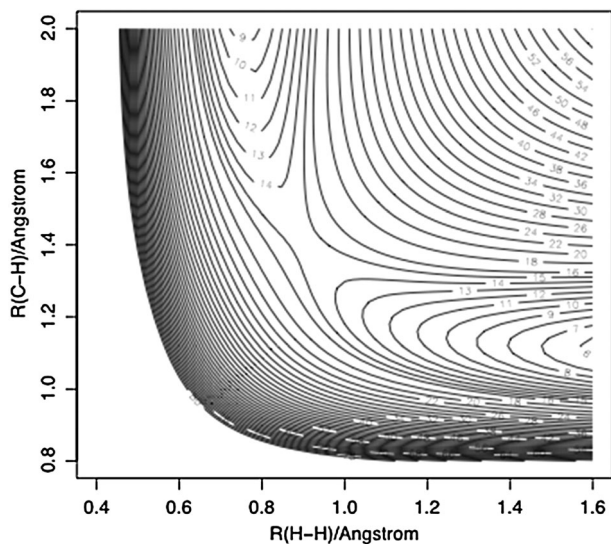


**Fig. 1** Equipotential (kcal/mol) contour plot of the H + CH<sub>4</sub> potential of ref. 44, as a function of the two reactive HH and CH bond lengths, with all other bond lengths fixed at the abstraction saddle point values.

reviewed in the next section. To close this section, we show in Fig. 1 an equipotential contour plot of the ZBB2 PES in the two reactive bond lengths  $r_{HH}$  and  $r_{CH}$  with the remaining ones held fixed at the abstraction saddle-point values. As seen, the contours are quite smooth. This is the expected result; however, it is worth pointing this out here because other fitting methods, which perform local fits and then use various interpolation methods of the fits, *e.g.*, Shepard interpolation, often result in slightly oscillatory equipotential contours.

### III. Reaction dynamics calculations

Global PESs, are of course needed for full-dimensional dynamics calculations, which can range in rigor from quantum, to semi-quantum or semi-classical to quasiclassical. The last

category is strictly classical and the “quasi” prefix simply refers to incorporating an approximate treatment of zero-point energy for the reactants, and often some assignment of quantum states to the products. The exact quantum treatment of reaction dynamics in full dimensionality is still a goal, not a reality, for more than four-atom systems. For tetraatomic reactions that proceed *via* formation of complexes, exact quantum methods are also still not practical. Reduced dimensionality quantum approaches,<sup>45–48</sup> which treat 2 to 7 degrees of freedom, are viable options and some of these will be described below. These approaches, which may not require full dimensional PESs (although obviously they can make use of them), may miss some key elements of the full-dimensional reaction dynamics, depending of course on the number of degrees of freedom treated. Semi-classical approaches, which are based on propagating exact classical trajectories, can be applied in full-dimensionality. However, these methods typically require a huge number of trajectories to converge the complex scattering amplitudes that they obtain. Thus, these methods are currently not in widespread use. This leaves the workhorse of the field, the quasiclassical trajectory method. This method is so well known that a review is neither necessary nor appropriate here. The interested reader is referred to reviews by Hase.<sup>49,50</sup> We have made extensive use of this method, and also made some extensions of it not found in these reviews; these will be described briefly below.

We next divide this section into four subsections, one on direct bimolecular reactions, a second on complex-forming bimolecular reactions, a third one on photochemically prepared unimolecular reactions, and the final one describing one electronically non-adiabatic reaction.

#### A. Direct bimolecular reactions

**H + CH<sub>4</sub>.** The H + CH<sub>4</sub> reaction has been the most thoroughly studied polyatomic direct reaction. It presents several challenges to theory and experiment and, not surprisingly, there have been many studies of the PES, the dynamics and the rate constant. This is also an interesting reaction also from the point of view of permutational symmetry where the order of the group is 5!

There are at least six full-dimensional PESs that have been reported for this system, an early one due to Jordan and Gilbert (JG),<sup>51</sup> which has a reaction barrier height roughly 4 kcal/mol below the correct value, two modifications of this surface,<sup>52,53</sup> a semi-global *ab initio* PES obtained by Shepard interpolation (scaled CCSD(T)/cc-pVTZ),<sup>54,55</sup> global *ab initio* ones we reported,<sup>43,44</sup> and most recently a global one also obtained by Shepard interpolation.<sup>56</sup> More details of these PESs will be given below. In addition, we note that Clary and coworkers have developed an *ab initio* reduced dimensional, two degree-of-freedom, PES for this reaction, which includes the local harmonic zero point energy in the remaining degrees of freedom.<sup>57</sup>

The rate of this reaction has been measured over the temperature range 300–2000 K. Because the barrier to reaction is roughly 15 kcal/mol, there is a large degree of tunneling at the lower end of this temperature range. Reproducing the rate constant,  $k(T)$ , in this end of the temperature range has been a

challenge for essentially exact and well-tested approximate methods. The challenge for exact methods is really the accuracy of the PES, and this is still unsettled. As discussed in detail by Manthe and coworkers,<sup>54,55</sup> who have performed benchmark, essentially exact calculations of  $k(T)$ , using  $J$ -shifting,<sup>46</sup> (which should be quite accurate for this system), agreement with experiment at temperatures below roughly 300 K is not yet satisfactory. This, despite using what is regarded as a highly accurate PES, based on semi-global Shepard interpolation. The PES has essentially the exact barrier height and harmonic normal-mode frequencies at the saddle point. Yet, the calculated rate constant is about a factor of two below experiment at 300 K. Above this temperature, agreement with experiment is quite satisfactory. It is possible that experiment has larger error bars than estimated at the lower temperatures where the rate constant is extremely small, *i.e.*, of the order of  $10^{-20}$  cm<sup>3</sup>/s.

It is interesting to note that a number of approximate calculations of  $k(T)$  are in better agreement with experiment than the benchmark ones mentioned above. However, none of these was done on the same PES used in the exact calculations and so this complicates the issue considerably. In this regard, it is important to note a second very important purpose of exact calculations, which is to serve as tests for approximate methods. Two very different, but approximate methods to obtain  $k(T)$  have been tested very recently for this reaction recently by Manthe and co-workers;<sup>58</sup> however, using the first modification of the JG PES, due to Espinosa-Garcia and denoted ES.<sup>52</sup> One is the Quantum Instanton method of Miller and co-workers, which was previously applied to this reaction using this PES.<sup>59</sup> This group reported very good agreement with experiment (fit to the data) down to 200 K. The other method tested is the widely-used canonical variational transition state theory with microcanonical optimized multi-dimensional (but 1d kinetic energy operator) tunneling, which was applied to this reaction by Pu and Truhlar.<sup>60</sup> These approximate methods were reported to be roughly 2.5–2.0 times larger than the benchmark  $k(T)$  in the temperature range 225–400 K. Very recently, Manolopoulos and co-workers<sup>61</sup> applied the semi-quantum “Ring Polymer Molecular Dynamics” method to obtain  $k(T)$  using the EG PES. The result was closer to the benchmark value in the above temperature range than the two approximate ones mentioned above, but still about a factor 1.8–1.5 larger than the benchmark  $k(T)$ . These comparisons with benchmark results are both very important and, it must be noted, very demanding, given the extremely small value of  $k(T)$  in this temperature range, *i.e.*,  $10^{-23}$  to  $10^{-21}$  cm<sup>3</sup>/s.

A number of reduced dimensionality quantum wavepacket calculations have been reported for the H + CH<sub>4</sub> reaction, using the ES PES. The largest of these were 6 and 7 degree-of-freedom ones (ref. 62 and 63, 64 respectively). These represent the current state-of-the-art in scattering calculations, although they typically are limited to initial-state resolved cross sections that are summed over all final states of the product. Very recent benchmark calculations of the initial state-resolved reaction probabilities using this PES have been used to test the results of these earlier calculations.<sup>65</sup> Both sets of reduced dimensionality results agreed well with the benchmark results for the one comparison given, *i.e.*, the energy

dependence of the reaction probability for the ground ro-vibrational state.

Cross sections for this reaction have been reported, both experimentally and theoretically. Zare and co-workers reported the energy dependence of the reaction cross section from the ground vibrational state of CH<sub>4</sub> and also CD<sub>4</sub> in the range 1.5–2.5 eV.<sup>8–10</sup> Schatz and coworkers performed quasi-classical trajectory AIMD B3LYP/DFT calculations of this cross-section and obtained reasonable agreement with experiment.<sup>8–10</sup> These calculations were done because the then-available PESs were not calibrated or fit to the potential in this high energy region and results using them were in disagreement with the AIMD ones. (It should be noted that B3LYP/DFT gives an inaccurately low barrier height and would produce a very inaccurate  $k(T)$ .)

Very recently, a joint experiment/theory paper<sup>56</sup> reported a comparison of the energy dependence of the reaction cross section for H + CD<sub>4</sub> over a wider collision energy range than reported in the earlier joint Zare-Schatz work. The new cross section was measured in a crossed-beam experiment using time-sliced velocity map ion-imaging techniques. It was calculated with a 7 degree-of-freedom wavepacket reactive scattering method and using the ZBB2 PES and also a new PES obtained with an extended Shepard interpolation method. Both PESs use the highly accurate CCSD(T)/aug-cc-pVTZ method and basis. The agreement between theory and experiment, including the earlier experimental result from the Zare group, shown in Fig. 2, is excellent, especially considering the small magnitude of the cross section. It is also gratifying to see that the two PESs produce virtually identical results.

The enhancement of the reaction cross section due to antisymmetric CH-stretch excitation in the reaction with CH<sub>4</sub> has been measured by Zare and co-workers,<sup>66,67</sup> at a collision energy of 1.52 eV. The enhancement factor was reported to be  $3.0 \pm 1.5$ . We<sup>68</sup> calculated this factor at this collision energy using the ZBB2 and ZBB3 PESs and obtained a value of 2–2.3, in good agreement with experiment.

We close this subsection on the H + CH<sub>4</sub> reaction by noting that the ZBB2 PES has also been used in a joint experimental

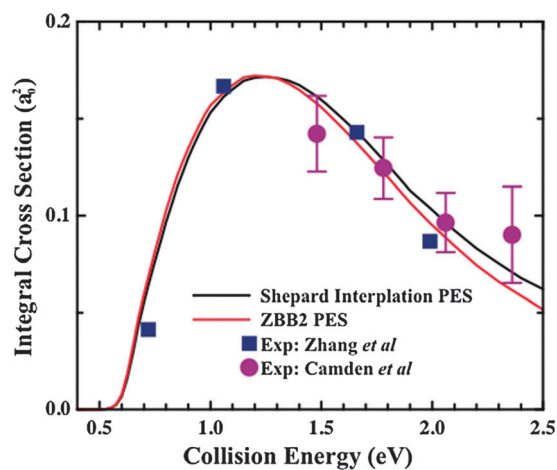


**Fig. 2** Experimental and calculated reaction cross section for the H + CD<sub>4</sub> → HD + CD<sub>3</sub> reaction as a function of the relative kinetic energy.

QCT study of the charge exchange reaction  $\text{CH}_5^+ + \text{Cs} \rightarrow [\text{CH}_5] \rightarrow \text{CH}_4 + \text{H}$ ,  $\text{CH}_3 + \text{H}_2$ <sup>69</sup> and mixed isotopologs.<sup>70</sup> In these calculations the initial zero-point phase space of the highly fluxional  $\text{CH}_5^+$ , which was obtained using an accurate PI PES,<sup>71</sup> was projected “vertically” onto the high energy portion of the  $\text{CH}_5$  ZBB2 PES and then trajectories were initiated there. Agreement with experiment was quite good for the branching ratios to the various products channels and also the translational energy distributions.

**F + CH<sub>4</sub>.** The F + CH<sub>4</sub> reaction is, like H + CH<sub>4</sub>, an H-atom abstraction reaction; however, the two reaction systems have more differences than similarities. F + CH<sub>4</sub> is very exoergic (−28 kcal/mol) and has a very low energy (roughly 0.5 kcal/mol) early barrier (reactant-like saddle point), whereas the H + CH<sub>4</sub> reaction is endoergic (3 kcal/mol) and its barrier is somewhat late and quite high (roughly 15 kcal/mol). Furthermore, the H<sub>3</sub>C–H–H saddle point has a collinear C–H–H bond arrangement, whereas high-level *ab initio* computations predict a bent H<sub>3</sub>C–H–F saddle-point structure with  $\angle(\text{CHF}) \approx 150^\circ$ .

The rate constant for this reaction has been reported,<sup>72–75</sup> most recently in 2006. As expected  $k(T)$  is much larger than the one for H + CH<sub>4</sub>; comparisons between theory and experiment for F + CH<sub>4</sub> are very much “a work in progress”, and will not be discussed here.

There have been detailed reactive scattering experiments on this reaction, in particular Nesbitt and co-workers<sup>76</sup> measured detailed HF( $v',j'$ ) ro-vibrational distributions at collision energy of 1.8 kcal/mol. They found that the HF product is vibrationally inverted and the most populated vibrational state is HF( $v' = 2$ ). Liu and co-workers measured correlated product vibrational distributions for the F + CH<sub>4</sub>( $v = 0$ ), F + CD<sub>4</sub>( $v = 0$ ), and F + CHD<sub>3</sub>( $v_1 = 0,1$ ) reactions at different collision energies in molecular beam experiments.<sup>77–82</sup>

The F + CH<sub>4</sub> reaction has been extensively studied theoretically as well. Several full- and reduced-dimensional PESs have been developed.<sup>83–88</sup> In 2007 Espinosa-García<sup>87</sup> reported the most recent semi-empirical PES, which was calibrated to reproduce the reaction energetics and the experimental thermal rate constant using variational transition state theory as implemented in the general polyatomic rate constants code POLYRATE.<sup>89</sup> An AIMD study was carried out by Troya<sup>90</sup> using the Specific Reaction Parameter method, briefly mentioned in the Introduction. Neither of these potentials had a realistic description of the entrance channel van der Waals well. Aoiz and co-workers<sup>86</sup> reported a “dual-level” Shepard-interpolated PES for this reaction and also carried out a careful *ab initio* analysis of the potential. They performed QCT calculations using two versions of the PES and the agreement with the Nesbitt and co-workers’ experiment<sup>76</sup> for the HF( $v',j'$ ) distributions was not good.

In 2009 we reported<sup>88</sup> a full-dimensional PI PES based on 19 384 UCCSD(T)/aug-cc-pVTZ quality *ab initio* energy points obtained by an efficient composite method employing explicit UCCSD(T)/aug-cc-pVDZ and UMP2/aug-cc-pVXZ [ $X = \text{D}, \text{T}$ ] computations. A schematic of the relevant energetics of the PES is given in Fig. 3. As seen it contains van der Waals minima both in the entrance and in the exit

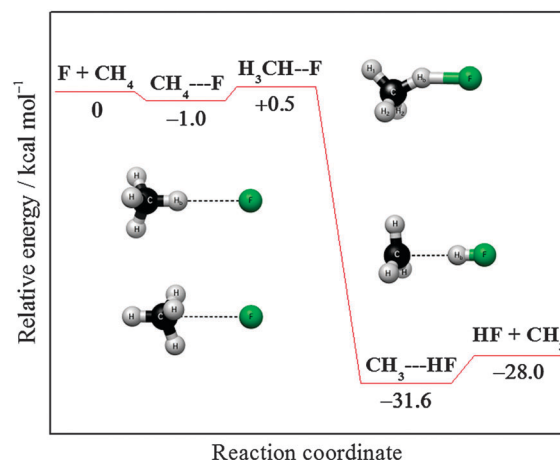


**Fig. 3** Energetics of the F + CH<sub>4</sub> → HF + CH<sub>3</sub> reaction relative to F + CH<sub>4</sub>(eq) as well as structures of the van der Waals complexes in the reactant channel, saddle point, and van der Waals complex in the product channel.

channels as well as a low energy first-order saddle-point separating the reactants from the products. The structures of these stationary points are also shown in Fig. 3.

We performed QCT calculations for the F + CH<sub>4</sub>( $v = 0$ ) reaction using the above-mentioned *ab initio* PES.<sup>88</sup> As Fig. 4 and 5 show the computed HF rotational-vibrational distributions are in excellent agreement with experiment superceding the accuracy of previous theoretical work. Thus, this study<sup>88</sup> demonstrated that QCT does reproduce measured product state distributions if an accurate PES is employed.

In 2009 a crossed-molecular beam experiment found that the CH stretching excitation in the F + CHD<sub>3</sub> reaction inhibits the breaking of the excited bond,<sup>81</sup> which questions our predictive chemical knowledge about mode-selective polyatomic reactivity. Conventional transition-state theory could not explain this surprising experimental result, since exciting the CH-stretch fundamental of CHD<sub>3</sub> decreases the ground-state vibrationally adiabatic barrier height.<sup>91,92</sup> In an even more recent experiment the effect of thermal bend excitation on the reaction was also investigated.<sup>93</sup> To study these effects, we performed millions of quasiclassical trajectories with these modes initially excited.<sup>91–93</sup> In order to do this in a QCT calculation we simply prepared the normal mode with  $\frac{3}{2}\hbar\omega_k$  of vibrational energy with all other modes in their ground vibrational state. Since classically this is not a stationary “state” it is necessary to monitor the conservation of the mode energy. This is shown for the CH-stretch and for the most reactive bend fundamental in CHD<sub>3</sub> in Fig. 6. As seen, the mode energies do stay well conserved, at least for a time-scale long enough to perform the QCT calculations.

As Fig. 7 shows the DF/HF product ratio increased with the CH-stretch excited at low  $E_{\text{coll}}$  relative to the ground state reaction, in agreement with experiment.<sup>81,91</sup> As a simple probe of the change in dynamics upon vibrational excitation and the dependence on  $E_{\text{coll}}$  we considered the “distance of closest” approach of the H or D to the F atom.<sup>91</sup> Following the pathway of all the trajectories we could assign both reactive and non-reactive trajectories to either the D<sub>3</sub>CH–F or D<sub>2</sub>HCD–F

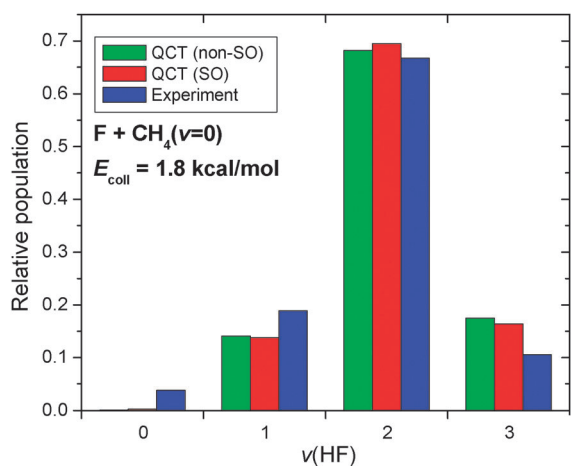


**Fig. 4** HF vibrational distributions obtained from QCT calculations using the non-SO PES from ref. 88 and the SO-corrected PES based on ref. 100. The QCT studies employ the same ZPE-constrained histogram binning as described in ref. 88. The experimental results are taken from ref. 76.

saddle-point configuration. As shown in Fig. 7 the F atom approaches one of the D atoms with much higher probability than statistically expected due to a long-range stereodynamical effect, which steers the slow F atom away from the vibrationally excited CH bond. The pre-reactive van der Waals well appears to be playing a role in this effect; however, a more detailed analysis of this is beyond the scope of this paper.

The effects of the bending mode excitations on this reaction has recently been reported in a joint theory/experiment paper.<sup>93</sup> The reactant bending-state-specific QCT calculations showed that the excitation of the  $\nu_5(e)$  bending-mode in  $\text{CHD}_3$  increases the cross sections the most efficiently and the  $\nu_5(e)$  mode excitation enhances the HF product channel as shown in Fig. 7 and 8. Furthermore, the experimental excitation functions of the  $\text{F} + \text{CHD}_3(\nu_b = 1) \rightarrow \text{HF}(\nu' = 3) + \text{CD}_3(\nu_2 = 0, 1)$  reaction displayed peak features indicating reactive resonances.<sup>93</sup> Such reactive resonances were seen in reduced-dimensional quantum computations.<sup>94,95</sup> Chu *et al.*<sup>94</sup> performed 5 degree-of-freedom quantum calculations using two new PESs and did observe a resonance from the ground

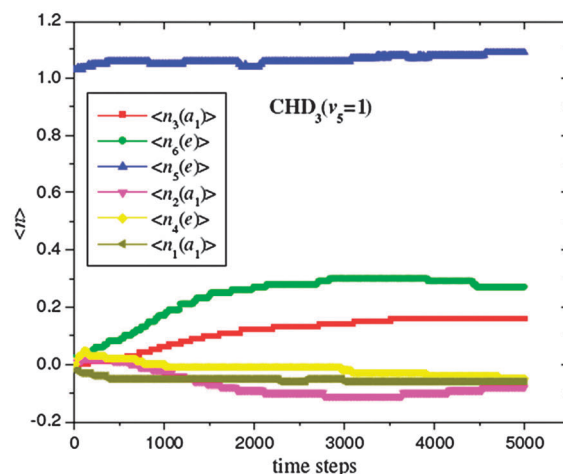
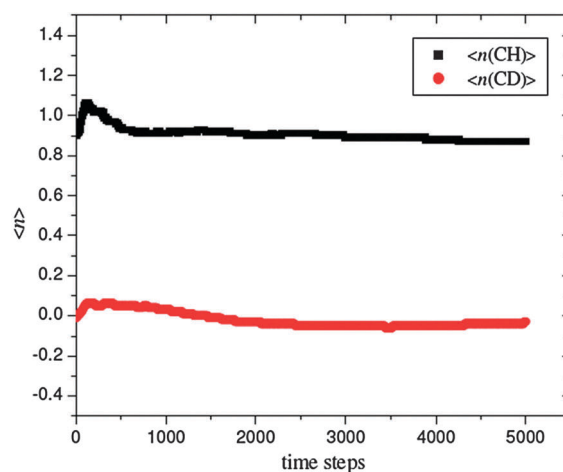


**Fig. 6** Expectation values of the harmonic vibrational quanta corresponding to the normal modes of CH-stretch-excited  $\text{CHD}_3(\nu_1 = 1)$  (upper panel) and bending-excited  $\text{CHD}_3(\nu_5 = 1)$  (lower panel) as a function of integration time. A time step is 0.0726 fs and the actions are averaged over 100 trajectories and the time interval  $[0, t]$ .

ro-vibrational state. But in later calculations using a newer PES, due to Espinosa-Garcia and co-workers,<sup>87</sup> Chu *et al.*<sup>95</sup> did not observe a resonance in the calculated integral cross

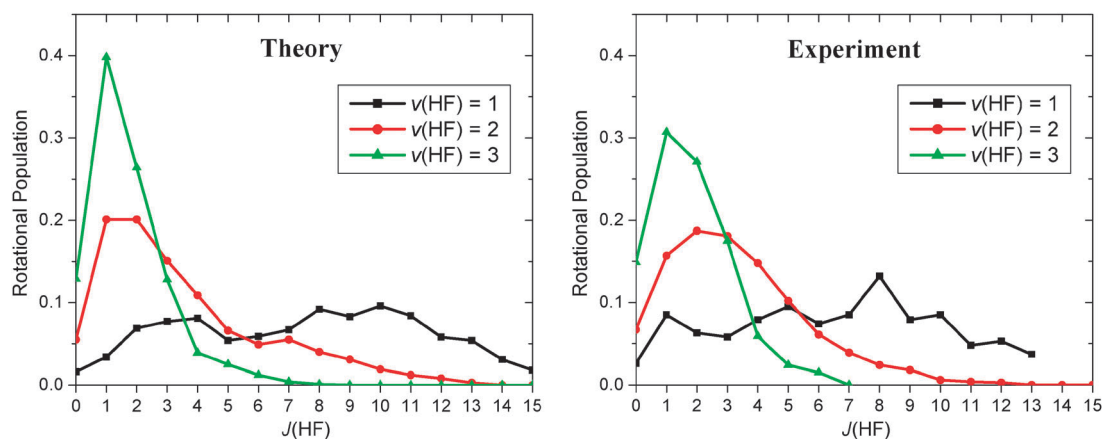


**Fig. 5** Rotational distributions for the HF product from the  $\text{F} + \text{CH}_4$  reaction at collision energy of 1.8 kcal/mol. The distributions are normalized for each vibrational state. Theoretical and experimental results are taken from ref. 88 and 76, respectively.

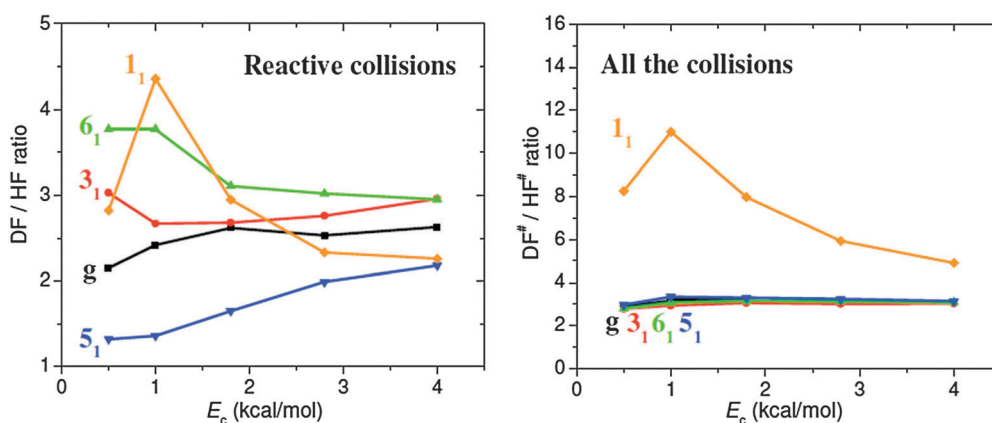


**Fig. 7** Computed reactant-vibrational-state-specific branching ratios of the reactive  $F + \text{CHD}_3$  collisions forming the DF and HF products (left panel). Ratios of the  $F + \text{CHD}_3$  trajectories (including the non-reactive ones as well) in which the F atom approaches either the D or H atom in the saddle-point region as a function of collision energy (right panel). g,  $1_1$ ,  $3_1$ ,  $5_1$ , and  $6_1$  denote the vibrational ground state and excitations by one quantum on the CH stretching and the three bending modes of  $\text{CHD}_3$ , respectively.

section from the ground ro-vibrational state of  $\text{CH}_4$ , but did not observe a resonance for the umbrella mode excited.

The detailed correlated measurements of the product state distributions present a major challenge to theory. Even reduced dimensionality quantum methods have not been attempted for this level of detail. QCT calculations can determine these; however, this requires the determination of the semi-classical quantum numbers of the products. For the present case, where the products are for example  $\text{HF} + \text{CD}_3$ , this is easy for the diatomic HF but not for  $\text{CD}_3$ . Following the early work of Schatz<sup>96</sup> and the more recent work of Espinosa-García,<sup>97</sup> we have developed a method for harmonic

normal-mode quantum number assignment for polyatomic products and the details are given elsewhere.<sup>92</sup>

Also, the question of how to bin the final states occurs and we have considered, in addition to the usual Histogram Binning, Gaussian Binning (GB).<sup>98</sup> However, the original GB method could not be efficiently employed for polyatomic products due to the exponential scaling of the number of required trajectories with the number of vibrational modes. Therefore, we proposed a modified GB approach based on the total vibrational energy together with Histogram Binning and employed this approach successfully for the  $\text{CD}_3$  and  $\text{CHD}_2$  products of the  $F + \text{CHD}_3$  reaction.<sup>92</sup> This procedure requires

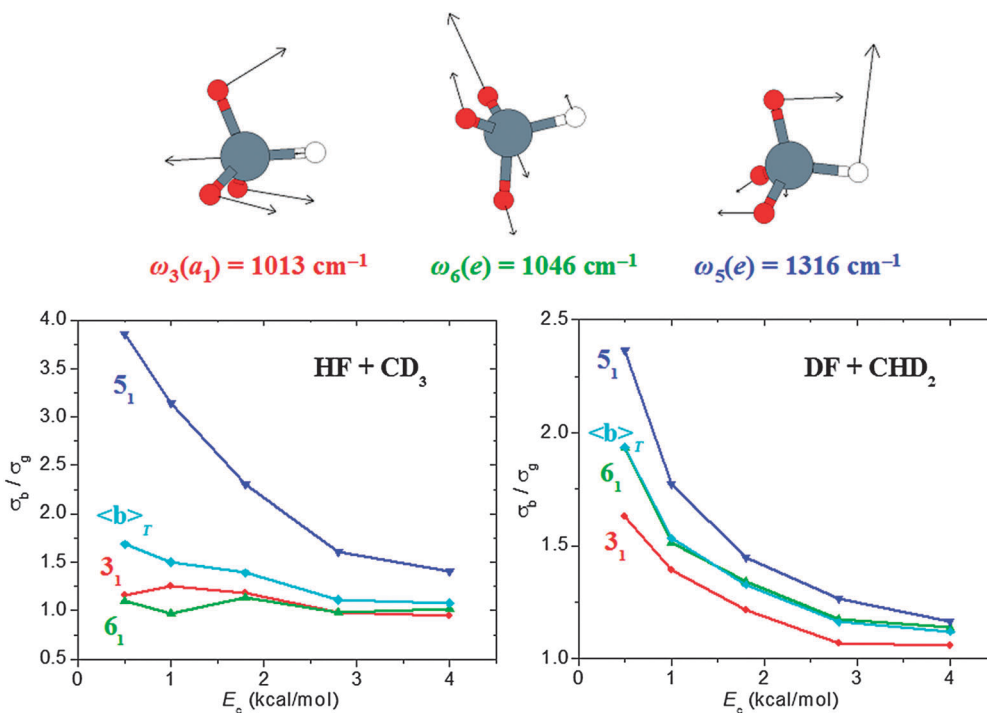


**Fig. 8** Computed reactant-bending-state-specific ratios of the total cross sections of the  $F + \text{CHD}_3(v_b = 1)$  and  $F + \text{CHD}_3(v = 0)$  reactions for the channels  $\text{HF} + \text{CD}_3$  and  $\text{DF} + \text{CHD}_2$  as a function of collision energy. The ratios denoted  $\langle b \rangle_r$  show the Boltzmann-weighted average of the bending-state-specific results at the vibrational temperature of 430 K.

only one Gaussian function for a polyatomic product, was recently denoted as 1GB by Bonnet and Espinosa-García,<sup>99</sup> who presented a theoretical argument supporting the proposed method.

Very recently, we proposed a spin-orbit (SO) correction to the F + CH<sub>4</sub> PES. The SO coupling plays important role in the entrance channel of the reaction and increases the barrier height significantly. As a consequence, the cross sections are smaller by a factor of 2–4 at low collision energies (~0.5 kcal/mol) if the QCTs are propagated on the SO ground state PES. The SO correction has virtually no effect on the product state distributions as shown in Fig. 4. These results are reported in detail elsewhere<sup>100</sup> in this themed issue.

Finally, we mention that the Cl + alkane (methane, ethane, etc) reactions have been also extensively studied both experimentally<sup>101–107</sup> and theoretically.<sup>108–115</sup> For the Cl + methane reaction several experimental investigations have been performed in the groups of Crim,<sup>101</sup> Zare,<sup>102,103</sup> and Liu<sup>104–107</sup> in order to study the effects of the reactant stretching and bending excitations. Unexpectedly, Liu and co-workers<sup>106</sup> found that the translational energy is more effective to drive the late-barrier Cl + CHD<sub>3</sub> reaction than the CH stretching excitation, contradicting to the Polanyi rules.<sup>116</sup> For further details on the Cl + alkane reactions the reader should consult the above references.

## B. Complex-forming bimolecular reactions

Examples of three reaction systems of the type for which *ab initio*-based global PI PESs have been developed using the methods of Section II are HO<sub>2</sub> + NO → OH + NO<sub>2</sub>, C(<sup>3</sup>P) + C<sub>2</sub>H<sub>2</sub> → C<sub>3</sub>H (linear and cyclic isomers) + H, C<sub>3</sub> + H<sub>2</sub> and H + HCO → H<sub>2</sub> + CO. Space does not permit as detailed discussion of these reactions as was done for H + CH<sub>4</sub> and F + CH<sub>4</sub>.

**HO<sub>2</sub> + NO.** The PI PES for the HO<sub>2</sub> + NO reaction was a fit to roughly 67 000 DFT-B3LYP/6-311G(*d, p*) energies.<sup>117</sup> A schematic of the stationary points is given in Fig. 9. The quality of the fit at the stationary points is good, as can be seen in Table 7, where comparisons of the PES energies with direct DFT-B3LYP/6-311G(*d, p*) ones. Highly accurate CCSD(T) results<sup>118</sup> are also there to assess the accuracy of the PES.

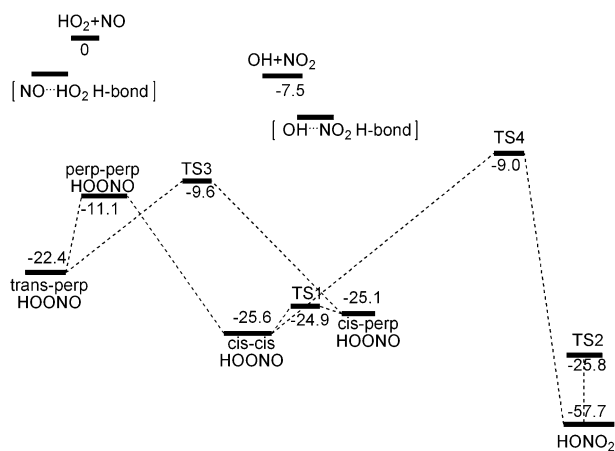


**Fig. 9** Schematic of full dimensional potential energy surface for HO<sub>2</sub> + NO reaction. Energies are in kcal/mol. See ref. 118 for structures of the some of the stationary points indicated.

**Table 7** Comparison of PES and indicated single-point electronic energies (kcal/mol) for the stationary points depicted in Fig. 9, relative to the HO<sub>2</sub> + NO minimum

	PES	CCSD(T)/CBS <sup>a</sup>	B3LYP/6-311G( <i>d,p</i> )
HO <sub>2</sub> + NO	0	0	0
OH + NO <sub>2</sub>	-7.5	-7.0	-6.4
HONO <sub>2</sub>	-57.6	-57.4	-56.6
<i>cis-cis</i>	-25.6	-30.6	-24.7
<i>Cis-perp</i>	-25.2		-23.5
<i>Trans-perp</i>	-22.3		-21.1
<i>Perp-perp</i>	-11.1		-9.6
TS1	-24.9		-23.5
TS2	-25.8		-25.7
TS3	-9.6		-8.9
TS4	-9.0	-7.2	
H-bond I	-5.3		-2.6
H-bond II	-6.5		-3.9

<sup>a</sup> Ref. 119.

The dynamics of this reaction to make OH + NO<sub>2</sub> is quite complex, as the atmospherically important isomers of HOONO as well as the more stable HONO<sub>2</sub> complex, are visited in the reaction. In addition, several high-energy H-bonded complexes play an important role in the overall reactivity. A complete discussion of this rich dynamics is beyond the scope of this Perspective and the interested reader is referred elsewhere<sup>117,118</sup> for such a discussion. Fig. 10 shows the time history of two trajectories, *i.e.*, the distance between

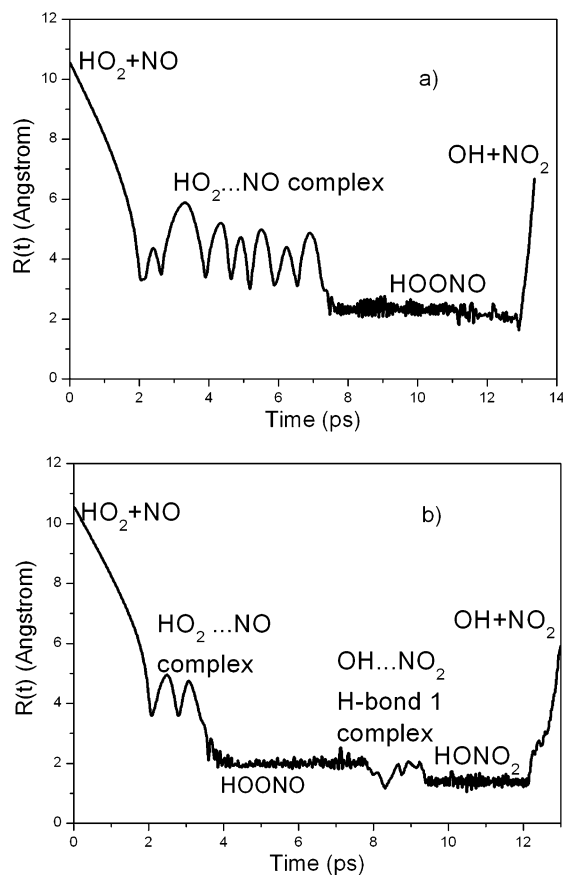


**Fig. 10** Time dependence of the distance between the centers of mass of HO<sub>2</sub> and NO for two complex-forming trajectories.

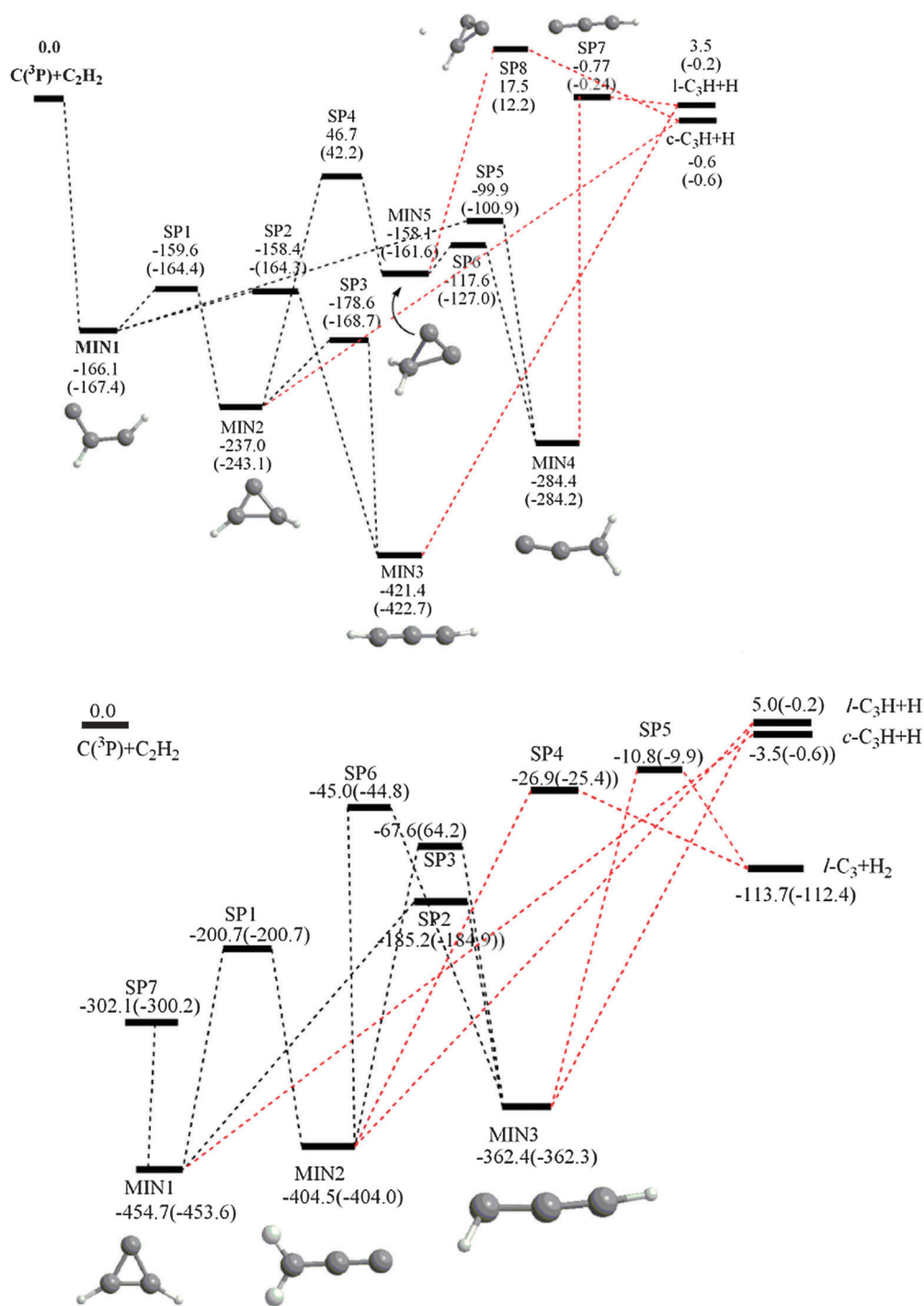


**Fig. 11** Schematic of singlet and triplet full-dimensional potential energy surface for C + C<sub>2</sub>H<sub>2</sub> reaction. Upper panel corresponds to the triplet surface and the lower panel to the singlet surface. Energies are in kJ/mol.

the centers of mass of HO<sub>2</sub> and NO, that exhibit some of this rich dynamics. As seen, in frame (a) the system first visits an H-bonded complex and then becomes temporarily trapped in the HOONO well and then goes on to make the products. In the presence of a third body the energized HOONO complex could be stabilized of course. In frame (b) HOONO isomerizes to HONO<sub>2</sub> by a very interesting “roaming” type mechanism, wherein HOONO nearly dissociates back to HO<sub>2</sub> + NO but instead returns to complex region, and forms HONO<sub>2</sub>.

**C(<sup>3</sup>P, <sup>1</sup>D) + C<sub>2</sub>H<sub>2</sub>.** The reaction C(<sup>3</sup>P) + C<sub>2</sub>H<sub>2</sub>, which has received considerable attention both in molecular beam experiments<sup>119–122</sup> and in scattering<sup>123–125</sup> and statistical calculations.<sup>126–128</sup> It is another example of a reaction that proceeds *via* several possible complexes and with several products that have been observed experimentally. There is great interest in the isomeric form of the C<sub>3</sub>H product (which can be in the nearly iso-energetic cyclic or linear forms). Also the C<sub>3</sub> product has been seen experimentally and this was

initially a bit of a puzzle. We constructed a global PI PES for the triplet reaction and a semi-global PI PES for the singlet reaction, using roughly 100 000 B3LYP/6-311g(*d,p*) energies for each PES.<sup>129</sup> The usual schematics of these PESs are given in Fig. 11; note the energies of the singlet PES are referenced to the same zero as the triplet PES, *i.e.*, C(<sup>3</sup>P) + C<sub>2</sub>H<sub>2</sub>(eq). We performed QCT calculations on both PESs and argued that the C<sub>3</sub> product probably is the result of intersystem crossing to the singlet PES followed by dissociation to that product and this is now the accepted mechanism. More details of this work can be found in ref. 129; however, we note that our study did not explicitly couple these surfaces.

Another example of reaction that involves singlet and triplet PESs that has been studied both experimentally<sup>130</sup> and theoretically<sup>11</sup> is O(<sup>3</sup>P) + C<sub>2</sub>H<sub>4</sub>. Schatz and co-workers<sup>11</sup> reported impressive spin-orbit-coupled-surface AIMD calculations on these two surfaces using DFT-B3LYP method with the 6-31G(*d, p*) basis. Owing to the large expense in doing these AIMD calculations, even with this very efficient method, the surface hopping method was simplified greatly, and 545 trajectories were generated, among which 143 trajectories were reactive. Propagation time for most trajectories was a maximum of 4000 steps (about 960 fs) although some trajectories were followed for 24 000 integration steps. Agreement with experiment on the major products formed was good, but the singlet to triplet branching ratio was not good. As pointed out more recently, the singlet and triplet states of this reaction, pose major challenges to electronic structure theory, especially in the biradical region.<sup>131</sup>

**H + HCO.** The H + HCO reaction to make H<sub>2</sub> + CO, is another example of a complex-forming reaction that we investigated,<sup>132</sup> which also exhibits a “roaming” pathway. This pathway will be discussed in more detail in the next subsection, where we review several unimolecular reactions.

### C. Unimolecular reactions

We now review several calculations of unimolecular dynamics using full-dimensional, global PI PESs for H<sub>2</sub>CO,<sup>132–138</sup> CH<sub>3</sub>CHO,<sup>139–143</sup> C<sub>3</sub>H<sub>5</sub>,<sup>42</sup> and CH<sub>2</sub>CH<sub>2</sub>OH.<sup>144</sup> Although these PESs also describe numerous bimolecular reactions, we place them under the “Unimolecular reactions” heading, because the corresponding experiments are photodissociation ones where the dynamics is unimolecular. In all cases these unimolecular reactions require roughly 10<sup>5</sup> or more propagations steps, because the trajectories are all initiated from the global minimum of the PES, where the initial photoexcitation takes place. This choice is certainly less biased than initiating trajectories at the conventional molecular saddle point for a specific product, which is typically done.

Also, as a result of making this choice, these calculations revealed surprising reaction pathways and here we give a brief review of the first two reactions, where the so-called “roaming” pathway to molecular products was uncovered.<sup>133,143</sup> This is a pathway that is quite “distant” from the conventional one, which occurs *via* a tight transition state saddle point that separates the relevant minimum, in these cases the global minimum and the molecular products, H<sub>2</sub> + CO and CH<sub>4</sub> + CO, respectively. The roaming pathway occurs in the incipient

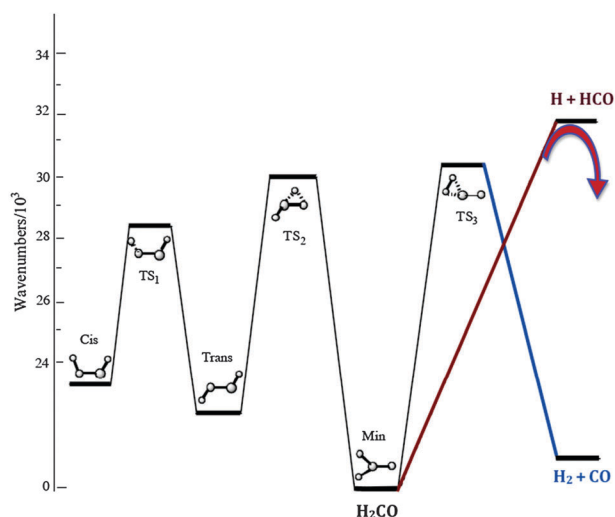


**Fig. 12** Schematic of singlet potential energy surface for H<sub>2</sub>CO, indicating the roaming pathway from incipient radical formation.

radical channel region, *i.e.*, H–HCO and CH<sub>3</sub>–HCO, respectively. This new pathway is indicated schematically in Fig. 12. One clear signature of roaming in this reaction that appears in experiment is shown in the CO rotational distribution following photodissociation. The calculated distribution is shown in Fig. 13 for two photolysis energies. At the lower energy the distribution is unimodal and peaked at around  $j_{\text{CO}} = 45$ . (This distribution can also be obtained by initiating trajectories at the conventional molecular saddle point.) The distribution at the higher energy shows a second peak at much lower  $j_{\text{CO}}$ . We showed that this peak is due to the roaming pathway, which also produces very highly vibrationally excited H<sub>2</sub>. This roaming pathway was first confirmed in joint experimental/theoretical work that appeared in 2004.<sup>133</sup> Much work has subsequently been reported on this and recent reviews<sup>134–136</sup> should be consulted for extensive results and discussion of this pathway. We do note that from the theoretical perspective, a global PES and the propagation of tens of thousands of trajectories were essential in order to make quantitative comparisons with experiment, which led to very firm conclusions about the roaming pathway and its consequences for experimental observables.

Shortly after roaming was reported in H<sub>2</sub>CO, it was also correctly speculated to occur in the photodissociation of CH<sub>3</sub>CHO to form the molecular products, CH<sub>4</sub> + CO.<sup>139</sup> Motivated by these experiments, we developed several global PESs for this very challenging system,<sup>141</sup> (Ohno and co-workers<sup>142</sup> have reported approximately 100 stationary points for the PES) and ran thousands of trajectories starting at the global minimum. The roaming pathway was determined to be the dominant pathway in these calculations. Frames of a trajectory that illustrate roaming are given in Fig. 14, where, as indicated the H-atom transfer for CH<sub>3</sub>–HCO occurs at a large CH distance of 3.9 Å. The resulting CH<sub>4</sub> is, not surprisingly, formed highly vibrationally excited. This prediction was verified later in a joint experimental/theoretical study of the CH<sub>4</sub> internal energy distribution.<sup>143</sup> In addition, the calculations predicted a much rotationally colder  $j_{\text{CO}}$ -distribution than the one predicted from initiating dynamics calculations at

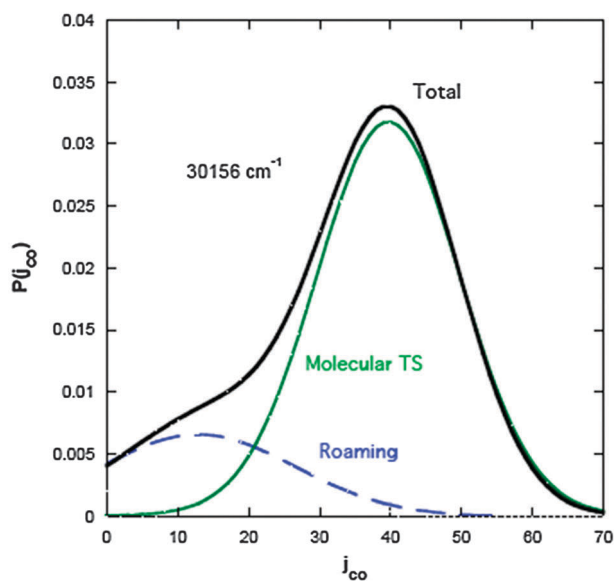
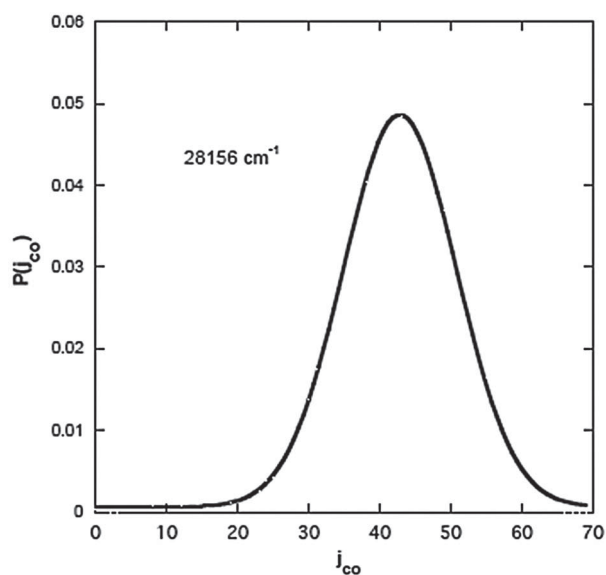


**Fig. 13** CO rotational energy distributions at photolysis energies indicated. See text for an explanation of the “Roaming” and “Molecular TS” components.

the conventional molecular channel saddle point. This dramatic difference is shown in Fig. 15, where the experimental distribution is also shown.

Very recently, several joint studies of unimolecular dissociation in  $C_3H_5$ <sup>42</sup> and  $CH_2CH_2OH$ <sup>144</sup> reported novel dynamical pathways, based on QCT calculations employing PI PESs for these high-dimensional systems. The reader is referred to references 42 and 144 for more details.

We conclude this subsection and introduce the next one by reminding the reader that the  $H_2CO$  and  $CH_3CHO$  photodissociation reactions involve three electronic states, the optically pumped  $S_1$  state, the “dark” lower energy  $T_1$  state and finally the  $S_0$  state, for which we have generated the PESs and performed the dynamics calculations. A rigorous dynamics description then should consider all three state and their couplings. Work on this for  $H_2CO$  is underway in our

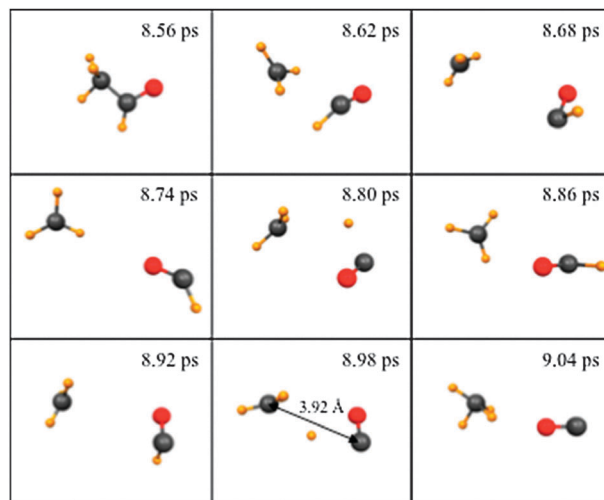


**Fig. 14** “Snapshots” of a roaming trajectory for  $CH_3CHO$  dissociation.

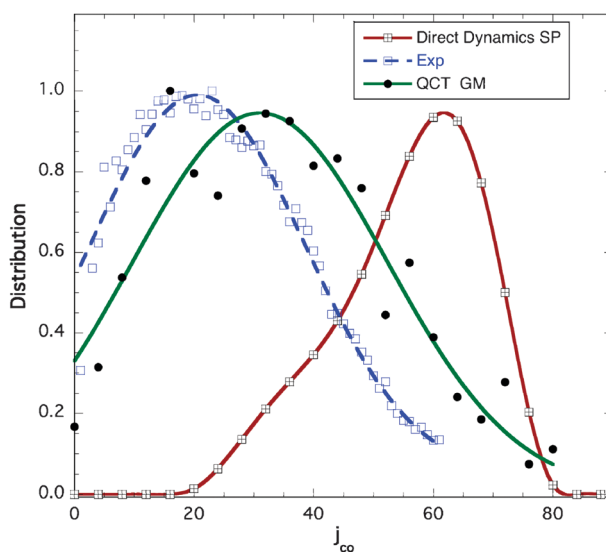


**Fig. 15** CO rotational energy distributions at 308 nm from experiment (ref. 139), quasiclassical trajectory calculations initiated at the global minimum (GM) and direct-dynamics calculations initiated at the conventional molecular saddle point.

group;<sup>145</sup> some limited dynamical investigations of the  $T_1/S_0$  surface crossings<sup>146</sup> and limited direct-dynamics wavepacket calculations of such processes have been reported by others.<sup>147</sup> However, these comments are meant mainly to introduce the last section on our recent calculations of the PESs and dynamics of the electronic quenching of  $OH^*$  by  $H_2$ .

#### D. Reactive and non-reactive electronic quenching of $OH^*$ by $H_2$

The electronic quenching of  $OH$  ( $A^2\Sigma^+$ ) by  $H_2(D_2)$  to  $OH + H_2(D_2)$  and  $H_2O + H$  ( $HDO + D$  and  $D_2O + H$ ) is an example of a bimolecular reaction where electronically non-adiabatic coupling is an essential part of the dynamics. This reaction has been studied experimentally by Lester and coworkers,<sup>148–154</sup> and Davis and coworkers.<sup>155</sup> Hoffman and Yarkony<sup>156</sup> reported configurations of thirteen conical

intersections (CoIs) for two planar and collinear symmetries. The energies of these CoIs vary from 2.8 to 3.3 eV, relative to  $\text{OH}(\text{eq}) + \text{H}_2(\text{eq})$ . Alexander and Lester and co-workers<sup>151</sup> reported potential energy surfaces of the ground and excited  $A'$  electronic states in two degrees of relevance to the  $\text{OH} + \text{H}_2$  products in the vicinity of the  $C_{2v}$  seam of intersections.

Developing global PESs for adiabatic states for this system using the fitting techniques described above is a major challenge. The reason for this is that the fitting bases we use cannot accurately describe the cusp-like properties of these adiabatic at CoIs. This is a well-known issue, and for this, and also for other reasons dealing with the non-adiabatic coupling elements, many workers in this field prefer to use a diabatic

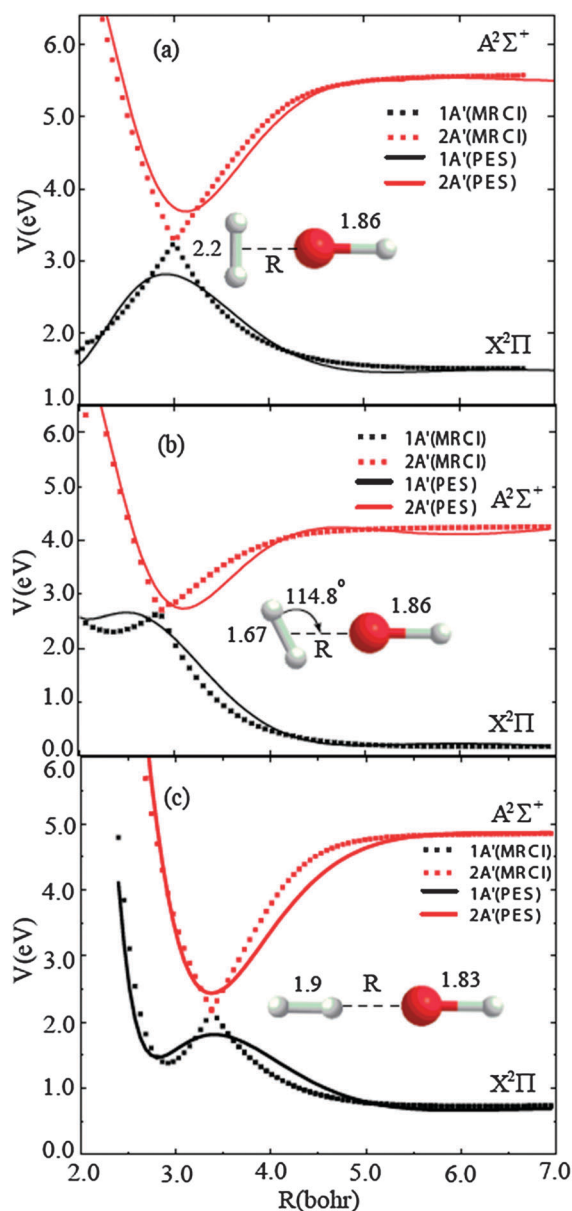


**Fig. 16** Comparison of electronic energies for the ground and electronically excited  $A'$  states of  $\text{OHH}_2$  at the two configurations indicated as  $R$  varies from the potential energy surfaces and direct *ab initio* calculations. Conical intersections occur for these configurations.

representation of the PESs instead of the adiabatic one. For fitting purposes, the diabatic representation is preferred because such PESs can be fit globally using the bases and fitting techniques we have described.

The above comments on fitting adiabatic PESs notwithstanding, we fit two adiabatic PI PESs relevant to this quenching reaction.<sup>157,158</sup> In planar geometries these PESs are of  $A'$  symmetry. Specifically we fit PI PESs to roughly 23 000 MRCI+Q/aug-cc-pVTZ electronic energies. Most of these configurations were determined by first running AIMD CASPT2/aug-cc-pVDZ calculations, initiated at or near the published 13 CoI geometries at the total energy of 4.46 eV.

As noted, the adiabatic PESs do not describe the cusp behavior at the CoIs, and this is illustrated in Fig. 16, which shows energies from the PESs and directly from *ab initio* calculations. As seen, the PES displays a rounded maximum and minimum for the  $1A'$  and  $2A'$  states, respectively. However, slightly away from the CoIs the PESs describe the MRCI energies very well. Similar comparisons for non-planar geometries are shown in Fig. 17, with OH and  $\text{H}_2$  internuclear distances fixed at 1.86 and 2.2 bohr, the indicated bond angle fixed at 170 degree, and with the dihedral angle  $\phi$  varying from 0 to 90 degrees. As seen, the PESs agree very well with the direct MRCI calculations. In summary, the PESs agree well the direct MRCI calculations except in the very limited region of the CoIs.

The QCT calculations we reported<sup>157–159</sup> did not consider the non-adiabatic derivative coupling between the PESs. Instead a very simple Franck–Condon-like procedure was used. That is, trajectories were initiated at each of the 13 CoIs and propagated on the ground state adiabatic PES. Initial momenta were selected microcanonically subject to the constraint of total energy. (Actually two types of microcanonical sampling were done; however, this is not relevant to this paper and more details can be found elsewhere.)<sup>157,158</sup> Both  $\text{H}_2\text{O} + \text{H}$  and  $\text{OH} + \text{H}_2$  products are formed with the former being dominant. Ro-vibrational distributions of the OH product have been reported by Lester and co-workers, and we show the comparison of the calculated distributions with experiment in Fig. 18. As seen, there is good agreement.

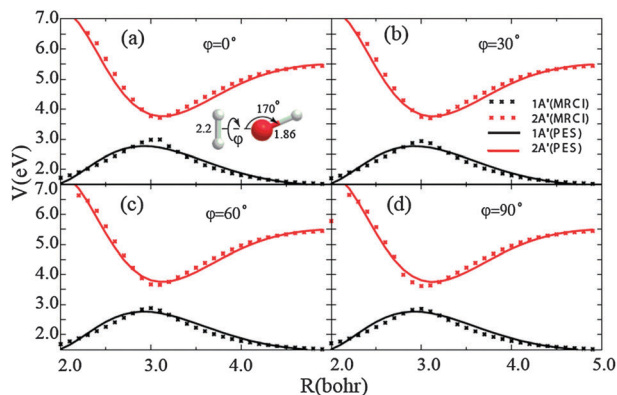


**Fig. 17** Comparison of electronic energies for the ground and electronically excited  $A'$  states of  $\text{OHH}_2$  at the two configurations indicated as  $R$  varies from the potential energy surfaces and direct *ab initio* calculations. Conical intersections do not occur for these configurations.

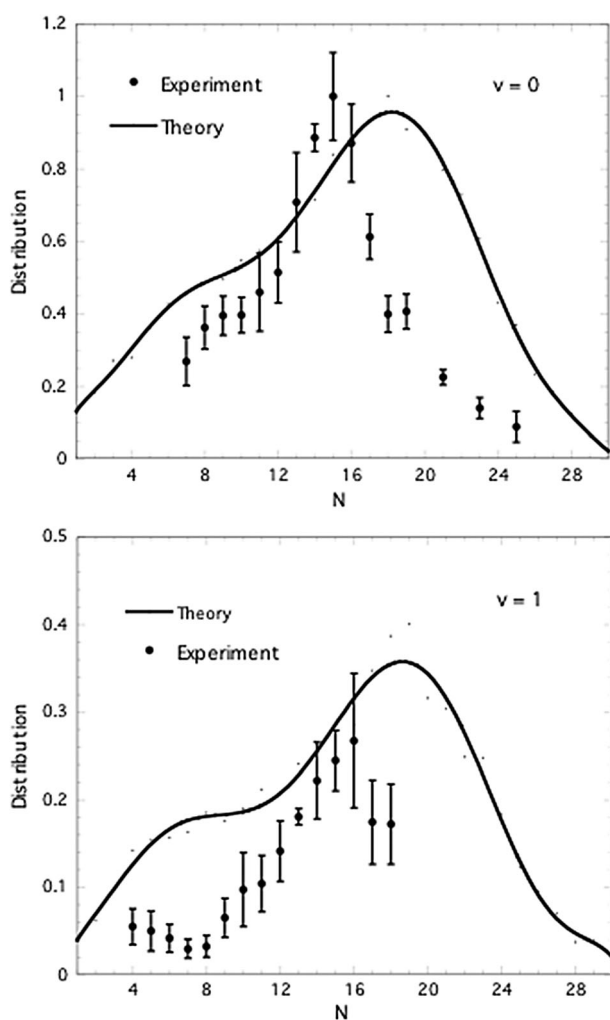


**Fig. 18** Comparison of calculated and experimental OH rotational distributions from OH\* + H<sub>2</sub> quenching for the indicated vibrational states.

In addition, we have predicted that the H<sub>2</sub>O product is formed highly vibrationally excited, with the bending mode in particular very excited. Hopefully this may stimulate experiments to investigate this.

As an aside, we note that the new PI PES for the ground electronic state reaction OH + H<sub>2</sub> → H<sub>2</sub>O + H is the most accurate one now available up to 4–5 eV. We have used it in studies of the high energy charge-exchange reaction H<sub>3</sub>O<sup>+</sup> + Cs → [H<sub>3</sub>O] → OH + H<sub>2</sub>, H<sub>2</sub>O + H,<sup>160</sup> using a similar “Franck–Condon” model briefly described above and in more detail elsewhere.<sup>69,70</sup>

Finally, we note that Han and co-workers have very recently reported diabatic potentials and couplings and quantum wavepacket calculations for coplanar OH\* + H<sub>2</sub> and D<sub>2</sub>.<sup>161,162</sup> These are impressive calculations and although a final state analysis of the H<sub>2</sub>O product was not done, the OH and H<sub>2</sub> ro-vibrational distributions were calculated. We have also calculated the OH ro-vibrational distribution with D<sub>2</sub> as the quenching partner<sup>158</sup> and find a peak at N = 17 in excellent agreement with the Han and co-workers’ wavepacket calculations.

#### IV. Summary, conclusions and final remarks

We have reviewed methods developed in our group to obtain potential energy surfaces in high dimensionality for chemical reactions. The PESs are explicitly invariant with respect to all permutations of identical atoms. This representation of the PES has enabled us to obtain precise fits for molecular systems with as many as ten atoms (24 internal degrees of freedom and 45 internuclear distances) with as “few” as 100 000 electronic energies. Illustrations of PESs and reaction dynamics were given to the H + CH<sub>4</sub>, F + CH<sub>4</sub>, HO<sub>2</sub> + NO, C + C<sub>2</sub>H<sub>2</sub>, H + HCO, OH\* + H<sub>2</sub> bimolecular reactions and H<sub>2</sub>CO and CH<sub>3</sub>CHO unimolecular reactions. In all cases the dynamics were done using the quasiclassical trajectory method, and the availability of a high quality PES enabled us to propagate many thousands of trajectories for hundreds of thousands of time steps. For unimolecular reactions the trajectories were initiated from the global minimum of the PES, instead of from the saddle-point corresponding to a given set of products, as is typically done, either in direct-dynamics calculations or using limited PESs. By initiating trajectories at the unbiased global minimum new dynamical roaming pathways to products were discovered.

There are many possible future applications of PI PESs; hopefully ones that will include quantum effects. Roaming for example, is perhaps a quantum mechanical resonance and there may be interesting quantum interferences between the roaming and conventional saddle-point pathways to the same products (same quantum state). Such calculations, while very challenging, will hopefully be realized in the not-too-distant future. Extending the fitting approach described here to more than 10 atoms should also be possible in the future; however, it may also be possible to combine the method that makes full use of permutational symmetry with direct-dynamics to develop more local fits. It may also be possible to use many-body decompositions of a large molecular system to represent the PES of hundreds of atoms. An example where this has been realized is for large water clusters.<sup>163</sup> Extending this approach to reactive PESs remains to be done.

#### Acknowledgements

We thank the Department of Energy and the National Science Foundation for financial support. We also thank our many collaborators, and especially Bastiaan Braams who developed the library of invariant polynomial bases.

#### References

- 1 J. M. Bowman and G. C. Schatz, *Annu. Rev. Phys. Chem.*, 1995, **46**, 169.
- 2 S. C. Althorpe and D. C. Clary, *Annu. Rev. Phys. Chem.*, 2003, **54**, 493.
- 3 D. Troya, M. J. Lakin and G. C. Schatz, *Modern Trends in Chemical Reaction Dynamics*, ed. X. M. Yang and K. Liu, World Scientific, Singapore, 2002 Advanced Series in Physical Chemistry, 14, pp. 249-90 (2004).
- 4 A. Sinha, M. C. Hsiao and F. F. Crim, *J. Chem. Phys.*, 1991, **94**, 4928.
- 5 M. J. Bronikowski, W. R. Simpson and R. N. Zare, *J. Phys. Chem.*, 1993, **97**, 2194.
- 6 W. Chen, W. L. Hase and H. B. Schlegel, *Chem. Phys. Lett.*, 1994, **228**, 436.

- 7 U. Lourderaj, K. Park and W. L. Hase, *Int. Rev. Phys. Chem.*, 2008, **27**, 361.
- 8 J. P. Camden, H. A. Bechtel, D. J. A. Brown, M. R. Martin, R. N. Zare, W. F. Hu, G. Lendvay, D. Troya and G. C. Schatz, *J. Am. Chem. Soc.*, 2005, **127**, 11898.
- 9 J. P. Camden, W. F. Hu, H. A. Bechtel, D. J. A. Brown, M. R. Martin, R. N. Zare, G. Lendvay, D. Troya and G. C. Schatz, *J. Phys. Chem. A*, 2006, **110**, 677.
- 10 W. F. Hu, G. Lendvay, D. Troya, G. C. Schatz, J. P. Camden, H. A. Bechtel, D. J. A. Brown, M. R. Martin and R. N. Zare, *J. Phys. Chem. A*, 2006, **110**, 3017.
- 11 W. Hu, G. Lendvay, B. Maiti and G. C. Schatz, *J. Phys. Chem. A*, 2008, **112**, 2093.
- 12 J. Zhou and H. B. Schlegel, *J. Phys. Chem. A*, 2009, **113**, 9958.
- 13 U. Lourderaj, K. Song, T. L. Windus, Y. Zhuang and W. L. Hase, *J. Chem. Phys.*, 2007, **126**, 044105.
- 14 H.-J. Werner, P. J. Knowles and R. D. Amos, *et al.*, MOLPRO, Version 2008.1, a package of *ab initio* programs.
- 15 A. González-Lafont, T. N. Truong and D. G. Truhlar, *J. Phys. Chem.*, 1991, **95**, 4618.
- 16 D. Troya, M. Mosch and K. A. O'Neill, *J. Phys. Chem. A*, 2009, **113**, 13863.
- 17 S. J. Greaves, A. J. Orr-Ewing and D. Troya, *J. Phys. Chem. A*, 2008, **112**, 9387.
- 18 D. Troya and E. Garcia-Molina, *J. Phys. Chem. A*, 2005, **109**, 3015.
- 19 A. Warshel and R. M. Weiss, *J. Am. Chem. Soc.*, 1980, **102**, 6218.
- 20 Y.-T. Chang and W. H. Miller, *J. Phys. Chem.*, 1990, **94**, 5884.
- 21 O. Tishchenko and D. G. Truhlar, *J. Chem. Phys.*, 2010, **132**, 084109.
- 22 G. C. Schatz, *Rev. Mod. Phys.*, 1989, **61**, 669.
- 23 T. Hollebeck, T. S. Ho and H. Rabitz, *Annu. Rev. Phys. Chem.*, 1999, **50**, 537.
- 24 C. Xu, D. Xie, P. Honvault, S. Y. Lin and H. Guo, *J. Chem. Phys.*, 2007, **127**, 024304.
- 25 M. A. Collins, *Theor. Chem. Acc.*, 2002, **108**, 313.
- 26 L. Zhang, P. Luo, Z. Huang, H. Chen and A. J. C. Varandas, *J. Phys. Chem. A*, 2008, **112**, 7238.
- 27 S. Manzhos and T. Carrington, *J. Chem. Phys.*, 2007, **127**, 12707.
- 28 R. Dawes, A. Passalacqua, A. F. Wagner, T. D. Sewell, M. Minkoff and D. L. Thompson, *J. Chem. Phys.*, 2009, **130**, 144107.
- 29 J. M. Bowman, B. J. Braams, S. Carter, C. Chen, G. Czako, B. Fu, X. Huang, E. Kamarchik, A. R. Sharma, B. C. Shepler, Y. Wang and Z. Xie, *J. Phys. Chem. Lett.*, 2010, **1**, 1866.
- 30 B. J. Braams and J. M. Bowman, *Int. Rev. Phys. Chem.*, 2009, **28**, 577.
- 31 J. N. Murrell, S. Carter, S. C. Farantos, P. Huxley and A. J. C. Varandas, *Molecular Potential Energy Functions*, John Wiley, Chichester, 1984.
- 32 J. M. Bowman and S.-L. Zou, *Chem. Phys. Lett.*, 2003, **368**, 421.
- 33 X.-B. Zhang, S.-L. Zou, L. B. Harding and J. M. Bowman, *J. Phys. Chem. A*, 2004, **108**, 8980.
- 34 A. Schmelzer and J. Murrell, *Int. J. Quantum Chem.*, 1985, **28**, 287.
- 35 P. Cassam-Chenaï and F. Patras, *J. Math. Chem.*, 2008, **44**, 938.
- 36 D. Opalka and W. J. Domcke, *J. Chem. Phys.*, 2010, **132**, 154108.
- 37 Z. Xie and J. M. Bowman, *J. Chem. Theory Comput.*, 2010, **6**, 26.
- 38 X. Huang, B. J. Braams and J. M. Bowman, *J. Chem. Phys.*, 2005, **122**, 044308.
- 39 H. Derksen and G. Kemper, *Computational Invariant Theory*, Springer Verlag, Berlin, Heidelberg, New York, 2002.
- 40 W. Bosma, J. Cannon and C. Playoust, *J. Symbolic Comput.*, 1997, **24**, 235.
- 41 Y. Wang, B. J. Braams, J. M. Bowman, S. Carter and D. P. Tew, *J. Chem. Phys.*, 2008, **128**, 224314.
- 42 C. Chen, B. Braams, D. Y. Lee, J. M. Bowman, P. L. Houston and D. Stranges, *J. Phys. Chem. Lett.*, 2010, **1**, 1875.
- 43 X. Zhang, B. J. Braams and J. M. Bowman, *J. Chem. Phys.*, 2006, **124**, 021104.
- 44 Z. Xie, J. M. Bowman and X. Zhang, *J. Chem. Phys.*, 2006, **125**, 133120.
- 45 J. M. Bowman, *Theor. Chem. Acc.*, 2002, **108**, 125.
- 46 J. M. Bowman, *J. Phys. Chem.*, 1991, **95**, 4960.
- 47 J. Z. H. Zhang, *Theory and Application of Quantum Molecular Dynamics*, World Scientific, Singapore, New Jersey, London, Hong Kong, 1999.
- 48 D. C. Clary, *Science*, 2008, **321**, 789.
- 49 W. L. Hase, *Classical Trajectory Simulations: Initial Conditions, a chapter in Encyclopedia of Computational Chemistry*, ed. N. L. Allinger, Wiley, New York, 1998, vol. 1, pp. 402–407.
- 50 W. L. Hase, *Classical Trajectory Simulations: Final Conditions, in Encyclopedia of Computational Chemistry*, ed. N. L. Allinger, Wiley, New York, 1998, vol. 1, pp. 399–402.
- 51 M. Jordan and R. Gilbert, *J. Chem. Phys.*, 1995, **102**, 5669.
- 52 J. Espinosa-García, *J. Chem. Phys.*, 2002, **116**, 10664.
- 53 J. C. Corchado, J. L. Bravo and J. Espinosa-García, *J. Chem. Phys.*, 2009, **130**, 184314.
- 54 T. Wu, H. J. Werner and U. Manthe, *Science*, 2004, **306**, 2227.
- 55 T. Wu, H. J. Werner and U. Manthe, *J. Chem. Phys.*, 2006, **124**, 164307.
- 56 W. Zhang, Y. Zhou, G. Wu, Y. Lu, H. Pan, B. Fu, Q. Shuai, L. Liu, S. Liu, L. Zhang, B. Jiang, D. Dai, S.-Y. Lee, Z. Xie, B. J. Braams, J. M. Bowman, M. A. Collins, D. H. Zhang and X. Yang, *Proc. Natl. Acad. Sci. U. S. A.*, 2010, **107**, 12782.
- 57 S. T. Banks, C. S. Tautermann, S. M. Remmert and D. C. Clary, *J. Chem. Phys.*, 2009, **131**, 044111.
- 58 S. Andersson, G. Nyman, A. Arnaldsson, U. Manthe and H. Jonsson, *J. Phys. Chem. A*, 2009, **113**, 4468.
- 59 Y. Zhao, T. Yamamoto and W. H. Miller, *J. Chem. Phys.*, 2004, **120**, 310.
- 60 J. Pu and D. G. Truhlar, *J. Chem. Phys.*, 2002, **117**, 1479.
- 61 Y. V. Suleimanov, R. Colleparado-Guevara and D. E. Manolopoulos, *Bimolecular reaction rates from ring polymer molecular dynamics: Application to  $H + CH_4 \rightarrow H_2 + CH_3$* , preprint.
- 62 D. Wang and J. M. Bowman, *J. Chem. Phys.*, 2001, **115**, 2055.
- 63 M. Yang, D. H. Zhang and S.-Y. Lee, *J. Chem. Phys.*, 2002, **117**, 9539.
- 64 M. Yang, S.-Y. Lee and D. H. Zhang, *J. Chem. Phys.*, 2007, **126**, 064303 and Y. Zhou and D. H. Zhang (unpublished), cited as ref. 35 in ref. 64.
- 65 G. Schiffel and U. Manthe, *J. Chem. Phys.*, 2010, **132**, 191101.
- 66 J. P. Camden, H. A. Bechtel, D. J. A. Brown and R. N. Zare, *J. Chem. Phys.*, 2005, **123**, 134301.
- 67 J. P. Camden, H. A. Bechtel, D. J. A. Brown and R. N. Zare, *J. Chem. Phys.*, 2006, **124**, 034311.
- 68 Z. Xie and J. M. Bowman, *Chem. Phys. Lett.*, 2006, **429**, 355.
- 69 J. E. Mann, Z. Xie, J. D. Savee, B. J. Braams, J. M. Bowman and R. E. Continetti, *J. Am. Chem. Soc.*, 2008, **130**, 3730.
- 70 J. E. Mann, Z. Xie, J. D. Savee, J. M. Bowman and R. E. Continetti, *J. Phys. Chem. A*, 2010, **114**, 11408.
- 71 Z. Jin, B. J. Braams and J. M. Bowman, *J. Phys. Chem. A*, 2006, **110**, 1569.
- 72 H. G. Wagner, J. Warnatz and C. Zetzsch, *Ann. Assoc. Quim. Argent.*, 1971, **59**, 169.
- 73 C. M. Moore, I. W. M. Smith and D. W. A. Stewart, *Int. J. Chem. Kinet.*, 1996, **26**, 813.
- 74 H. Kornweitz, A. Persky and R. D. Levine, *Chem. Phys. Lett.*, 1998, **289**, 125.
- 75 A. Persky, *Chem. Phys. Lett.*, 2006, **430**, 251.
- 76 W. W. Harper, S. A. Nizkorodov and D. J. Nesbitt, *J. Chem. Phys.*, 2000, **113**, 3670.
- 77 J. Zhou, J. J. Lin and K. Liu, *J. Chem. Phys.*, 2004, **121**, 813.
- 78 J. J. Lin, J. Zhou, W. Shiu and K. Liu, *Science*, 2003, **300**, 966.
- 79 J. Zhou, J. J. Lin, W. Shiu, S.-C. Pu and K. Liu, *J. Chem. Phys.*, 2003, **119**, 2538.
- 80 J. Zhou, J. J. Lin and K. Liu, *J. Chem. Phys.*, 2003, **119**, 8289.
- 81 W. Zhang, H. Kawamata and K. Liu, *Science*, 2009, **325**, 303.
- 82 J. Zhou, J. J. Lin, B. Zhang and K. Liu, *J. Phys. Chem. A*, 2004, **108**, 7832.
- 83 J. C. Corchado and J. Espinosa-García, *J. Chem. Phys.*, 1996, **105**, 3160.
- 84 D. Troya, J. Millan, I. Banos and M. Gonzalez, *J. Chem. Phys.*, 2004, **120**, 5181.
- 85 C. Rángel, M. Navarrete and J. Espinosa-García, *J. Phys. Chem. A*, 2005, **109**, 1441.
- 86 J. F. Castillo, F. J. Aoiz, L. Banares, E. Martinez-Nunez, A. Fernandez-Ramos and S. Vazquez, *J. Phys. Chem. A*, 2005, **109**, 8459.
- 87 J. Espinosa-García, J. L. Bravo and C. Rangel, *J. Phys. Chem. A*, 2007, **111**, 2761.
- 88 G. Czako, B. C. Shepler, B. J. Braams and J. M. Bowman, *J. Chem. Phys.*, 2009, **130**, 084301.

- 89 J. C. Corchado, Y.-Y. Chuang, P. L. Fast, J. Villa, W.-P. Hu, Y.-P. Liu, G. C. Lynch, K. A. Nguyen, C. F. Jackels, V. S. Melissas, B. J. Lynch, I. Rossi, E. L. Coitino, A. Fernandez-Ramos, R. Steckler, B. C. Garrett, A. D. Isaacson and D. G. Truhlar, *POLYRATE*, University of Minnesota, Minneapolis, MN, 2000.
- 90 D. Troya, *J. Chem. Phys.*, 2005, **123**, 214305.
- 91 G. Czako and J. M. Bowman, *J. Am. Chem. Soc.*, 2009, **131**, 17534.
- 92 G. Czako and J. M. Bowman, *J. Chem. Phys.*, 2009, **131**, 244302.
- 93 G. Czako, Q. Shuai, K. Liu and J. M. Bowman, *J. Chem. Phys.*, 2010, **133**, 131101.
- 94 T. S. Chu, X. Zhang, L. P. Ju, L. Yao, K. L. Han, M. L. Wang and J. Z. H. Zhang, *Chem. Phys. Lett.*, 2006, **424**, 243.
- 95 T. Chu, K. Han and J. Espinosa-Garcia, *J. Chem. Phys.*, 2009, **131**, 244303.
- 96 G. C. Schatz, *Molecular Collision Dynamics*, ed. J. M. Bowman, Springer-Verlag, Berlin, 1983, pp. 25–60.
- 97 J. C. Corchado and J. Espinosa-Garcia, *Phys. Chem. Chem. Phys.*, 2009, **11**, 10157.
- 98 L. Bonnet and J. C. Rayez, *Chem. Phys. Lett.*, 1997, **277**, 183.
- 99 L. Bonnet and J. Espinosa-Garcia, *J. Chem. Phys.*, 2010, **133**, 164108.
- 100 G. Czako and J. M. Bowman, *Phys. Chem. Chem. Phys.*, 2011, DOI: 10.1039/c0cp02456b.
- 101 R. J. Holiday, C. H. Kwon, C. J. Annesley and F. F. Crim, *J. Chem. Phys.*, 2006, **125**, 133101.
- 102 S. A. Kandel and R. N. Zare, *J. Chem. Phys.*, 1998, **109**, 9719.
- 103 H. A. Bechtel, J. P. Camden, D. J. A. Brown, M. R. Martin, R. N. Zare and K. Vodopyanov, *Angew. Chem., Int. Ed.*, 2005, **44**, 2382.
- 104 J. Zhou, J. J. Lin, B. Zhang and K. Liu, *J. Phys. Chem. A*, 2004, **108**, 7832.
- 105 B. Zhang and K. Liu, *J. Phys. Chem. A*, 2005, **109**, 6791.
- 106 S. Yan, Y.-T. Wu, B. Zhang, X.-F. Yue and K. Liu, *Science*, 2007, **316**, 1723.
- 107 S. Yan, Y.-T. Wu and K. Liu, *Proc. Natl. Acad. Sci. U. S. A.*, 2008, **105**, 12667.
- 108 H.-G. Yu and G. Nyman, *Phys. Chem. Chem. Phys.*, 1999, **1**, 1181.
- 109 J. C. Corchado, D. G. Truhlar and J. Espinosa-Garcia, *J. Chem. Phys.*, 2000, **112**, 9375.
- 110 S. Skokov and J. M. Bowman, *J. Chem. Phys.*, 2000, **113**, 4495.
- 111 J. Sanson, J. C. Corchado, C. Rangel and J. Espinosa-Garcia, *J. Chem. Phys.*, 2006, **124**, 074312.
- 112 J. Sanson, J. C. Corchado, C. Rangel and J. Espinosa-Garcia, *J. Phys. Chem. A*, 2006, **110**, 9568.
- 113 J. Palma and D. C. Clary, *J. Chem. Phys.*, 2000, **112**, 1859.
- 114 H.-G. Yu and G. Nyman, *J. Chem. Phys.*, 2000, **112**, 238.
- 115 S. J. Greaves, J. Kim, A. J. Orr-Ewing and D. Troya, *Chem. Phys. Lett.*, 2007, **441**, 171.
- 116 J. C. Polanyi, *Science*, 1987, **236**, 680.
- 117 C. Chen, B. C. Shepler and J. M. Bowman, *Phys. Chem. Chem. Phys.*, 2009, **11**, 4722.
- 118 C. Chen, B. C. Shepler, B. J. Braams and J. M. Bowman, *J. Chem. Phys.*, 2007, **127**, 104310.
- 119 D. A. Dixon, D. Feller, C. Zhan and J. S. Francisco, *J. Phys. Chem. A*, 2004, **106**, 3191.
- 120 R. I. Kaiser, A. M. Mebel and Y. T. Lee, *J. Chem. Phys.*, 2001, **114**, 231.
- 121 F. Leonori, R. Petrucci, E. Segoloni, A. Bergeat, K. M. Hickson, N. Balucani and P. Casavecchia, *J. Phys. Chem. A*, 2008, **112**, 1363.
- 122 M. Costes, P. Halvick, K. M. Hickson, N. Daugey and C. Naulin, *Astrophys. J.*, 2009, **703**, 1179.
- 123 R. Guadagnini, G. C. Schatz and S. P. Walch, *J. Phys. Chem. A*, 1998, **102**, 5857.
- 124 A. M. Mebel, W. M. Jackson, A. H. H. Chang and S. H. Lin, *J. Am. Chem. Soc.*, 1998, **120**, 5751.
- 125 C. F. Williams, S. K. Pogrebnya and D. C. Clary, *J. Chem. Phys.*, 2007, **126**, 154321.
- 126 D. C. Clary, E. Buonomo, I. R. Sims, I. W. M. Smith, W. D. Geppert, C. Naulin, M. Costes, L. Cartechini and P. Casavecchia, *J. Phys. Chem. A*, 2002, **106**, 5541.
- 127 E. Buonomo and D. C. Clary, *J. Phys. Chem. A*, 2001, **105**, 2694.
- 128 T. Takayanagi, *J. Phys. Chem. A*, 2006, **110**, 361.
- 129 W. K. Park, J. Park, S. C. Park, B. J. Braams, C. Chen and J. M. Bowman, *J. Chem. Phys.*, 2006, **125**, 081101.
- 130 P. Casavecchia, G. Capozza, E. Segoloni, F. Leonori, N. Balucani and G. G. Volpi, *J. Phys. Chem. A*, 2005, **109**, 3527.
- 131 A. C. West, J. S. Kretschmer, B. Sellner, K. Park, W. L. Hase, H. Lischka and T. L. Windus, *J. Phys. Chem. A*, 2009, **113**, 12663.
- 132 K. Christoffel and J. M. Bowman, *J. Phys. Chem. A*, 2009, **113**, 4138.
- 133 S. A. Lahankar, S. K. Lee, S. D. Chambreau, A. G. Suits, X. Zhang, J. Rheinecker, L. B. Harding and J. M. Bowman, *Science*, 2004, **306**, 1158.
- 134 J. M. Bowman and X. Zhang, *Phys. Chem. Chem. Phys.*, 2006, **8**, 321.
- 135 A. G. Suits, *Acc. Chem. Res.*, 2008, **41**, 783.
- 136 J. M. Bowman and B. C. Shepler, *Ann. Rev. Phys. Chem.*, 2011, **62**, 531–553.
- 137 S. A. Lahankar, S. D. Chambreau, D. Townsend, F. Suits, J. Farnum, X. Zhang, J. M. Bowman and A. G. Suits, *J. Chem. Phys.*, 2006, **125**, 044303.
- 138 X. Zhang, J. L. Rheinecker and J. M. Bowman, *J. Chem. Phys.*, 2005, **122**, 114313.
- 139 P. L. Houston and S. H. Kable, *Proc. Natl. Acad. Sci. U. S. A.*, 2006, **103**, 16079.
- 140 J. M. Bowman, *Proc. Natl. Acad. Sci. U. S. A.*, 2006, **103**, 16061.
- 141 B. C. Shepler, B. J. Braams and J. M. Bowman, *J. Phys. Chem. A*, 2008, **112**, 9344.
- 142 X. Yang, S. Maeda and K. Ohno, *J. Phys. Chem. A*, 2007, **111**, 5099.
- 143 B. R. Heazlewood, M. J. T. Jordan, S. H. Kable, T. M. Selby, D. L. Osborn, B. C. Shepler, B. J. Braams and J. M. Bowman, *Proc. Natl. Acad. Sci. U. S. A.*, 2008, **105**, 12719.
- 144 E. Kamarchik, L. Koziol, H. Reisler, J. M. Bowman and A. I. Krylov, *J. Phys. Chem. Lett.*, 2010, **1**, 3058.
- 145 B. Fu, B. C. Shepler and J. M. Bowman, in preparation.
- 146 B. C. Shepler, E. Epifanovsky, P. Zhang, J. M. Bowman, A. I. Krylov and K. Morokuma, *J. Phys. Chem. A*, 2008, **112**, 13267.
- 147 M. Araújo, B. Lasorne, A. L. Magalhães, G. A. Worth, M. J. Bearpark and M. A. Robb, *J. Chem. Phys.*, 2009, **131**, 144301.
- 148 D. T. Anderson, M. W. Todd and M. I. Lester, *Annu. Rev. Phys. Chem.*, 1999, **110**, 11117.
- 149 M. W. Todd, D. T. Anderson and M. I. Lester, *J. Phys. Chem. A*, 2001, **105**, 10031.
- 150 B. Pollack, Y. Lei, T. A. Stephenson and M. I. Lester, *Chem. Phys. Lett.*, 2006, **421**, 324.
- 151 P. A. Cleary, L. P. Dempsey, C. Murray, M. I. Lester, J. Klos and M. H. Alexander, *J. Chem. Phys.*, 2007, **126**, 204316.
- 152 L. P. Dempsey, P. A. Cleary, C. Murray and M. I. Lester, *J. Chem. Phys.*, 2007, **127**, 151101.
- 153 L. P. Dempsey, C. Murray, P. A. Cleary and M. I. Lester, *Phys. Chem. Chem. Phys.*, 2008, **10**, 1424.
- 154 L. P. Dempsey, T. D. Sechler, C. Murray, M. I. Lester and S. Matsika, *J. Chem. Phys.*, 2009, **130**, 104307.
- 155 M. Ortiz-Suarez, M. F. Witinski and H. F. Davis, *J. Chem. Phys.*, 2006, **124**, 201106.
- 156 B. C. Hoffman and D. R. Yarkony, *J. Chem. Phys.*, 2000, **113**, 10091.
- 157 E. Kamarchik, Bina Fu and J. M. Bowman, *J. Chem. Phys.*, 2010, **132**, 091102.
- 158 B. Fu, E. Kamarchik and J. M. Bowman, *J. Chem. Phys.*, 2010, **133**, 164306.
- 159 J. H. Lehman, L. P. Dempsey, M. I. Lester, B. Fu, E. Kamarchik and J. M. Bowman, *J. Chem. Phys.*, 2010, **133**, 164307.
- 160 J. E. Mann, Z. Xie, J. D. Savee, J. M. Bowman and R. Continetti, *J. Chem. Phys.*, 2009, **130**, 041102.
- 161 P. Y. Zhang, R. F. Lu, T. S. Chu and K. L. Han, *J. Phys. Chem. A*, 2010, **114**, 6565.
- 162 P. Y. Zhang, R. F. Lu, T. S. Chu and K. L. Han, *J. Chem. Phys.*, 2010, **133**, 174316.
- 163 Y. Wang and J. M. Bowman, *Chem. Phys. Lett.*, 2010, **491**, 1.
- 164 Y. Wang, J. M. Bowman and X. Huang, *J. Chem. Phys.*, 2010, **133**, 111103.
- 165 A. R. Sharma, B. J. Braams, S. Carter, B. C. Shepler and J. M. Bowman, *J. Chem. Phys.*, 2009, **130**, 17430.
- 166 Z. Xie, B. J. Braams and J. M. Bowman, *J. Chem. Phys.*, 2005, **122**, 224307.